

Republic of Iraq
Ministry of Higher Education and Scientific Research
University of Babylon
College of Science for Women
Department of Laser Physics



A Study on the Surface Plasmon Effects on the Optical Properties of Light-Emitting Polymers

A Thesis

Submitted to the Council of the College of Science for Women / University of Babylon in Partial Fulfillment of the Requirements for the Master Degree in Laser Physics

By

Zainab Adnan Abdul Mahdi

B.Sc. Physics laser 2019

Supervised by

Assist. Prof. Dr. Nizar Salem Shanan

Assist. Prof. Dr. Ahmed Kadem Kodeary

بِسْمِ اللَّهِ الرَّحْمَنِ الرَّحِيمِ

﴿وَلَمَّا بَلَغَ أَشُدَّهُ آتَيْنَاهُ حُكْمًا

وَعِلْمًا وَكَذَلِكَ نَجْزِي الْمُؤْمِنِينَ﴾

صدق الله العظيم

سورة يوسف (22)

Dedication

To the one who stood beside me and stayed up the nights and was patience to get to where I am (my mother) may Allah perpetuate her as an asset.

To the one who supported me and was never stingy with anything (my father), may A protect him.

To that who in light the way to me and support me (my brother), may Allah grant it success.

To the comfort of my soul, good companionship and lasting love... my friend (Ghufran Hadi).

Dedicate the results of this research to them

Zainab

Acknowledgments

*First, I should like to express my deep thanks to the Almighty , ALLAH JALA JALALAH, for what I have been. I would like to express my deep gratitude and appreciation to my supervisors Assist. Prof. Dr. **Nizar Salim Shnan** and Assist Prof. Dr. **Ahmed Kadem Kodeaey** for suggesting the topic of the thesis, continuous advice and their guidance throughout this work,*

*I am also greatly indebted to the staff of the laser physics department in the College of Science for Women University of Babylon for their continuous support specially Mr. **Rafia Tohma**.*

*As I Would like to thank Assist Prof. Dr **Saddam Haddawi** for providing assistance and continuous support.*

And not last, I Would like to thank everyone helped me any way to obtain the present

Abstract

A Light-Emitting Polymers (LEPs) are materials that absorb light at one wavelength and emit it at another. They are crucial for applications like LEDs and displays. Mixing LEPs with plasmonic metal nanoparticles enhances their optical properties through plasmon-exciton coupling. This phenomenon boosts light emission efficiency, allows precise control of emitted light, and improves overall optoelectronic device performance.

The present experimental study focused on improving the optical properties of the LEPs by doping them with a plasmonic metal nanoparticles. To achieve this purpose, two types of the LEPs were used MEH-PPV and PFO, which are dissolved with an organic solvent (Toluene) at different concentrations. In addition, gold nanoparticles (Au NPs) and silver nanoparticles (Ag NPs) were synthesized by pulsed laser ablation in liquids (PLAL) method with nanosecond laser pulses at 1064 nm. The average size of the Au NPs and the Ag NPs, which were experimentally created from 18 to 35 nm.

To obtain improved optical properties, the MEH-PPV polymer is mixed with the Au NPs at different concentrations, while the PFO polymer is mixed with the Ag NPs at different concentrations.

The optical absorption was measured using a UV–Vis spectrophotometer, the fluorometer, and laser induced fluorescence (LIF) technique for all samples.

The results revealed adjustable optical properties for both LEPs by controlling the concentration of nanoparticles, which are added to the LEPs. Optimal emission was observed at a nanoparticle concentration of 500 pulses.

Accordingly, the results show the possibility of using the enhanced LEPs in many applications, especially in the development of optical devices and detectors.

List of Contents

Section	Subject	Page No.
Chapter one : Introduction		
(1-1)	Introduction	1
(1-2)	Literature review	4
(1-3)	Aim of the Work and Research Motivation	11
Chapter two : Theoretical Part		
(2-1)	Introduction	12
(2-2)	Surface Plasmon Resonance	12
(2-2-1)	Surface Plasmon Polariton	13
(2-2-2)	Localized Surface Plasmon	14
(2-3)	Excitons	17
(2-4)	Exciton-plasmon coupling	18
(2-5)	linear optical properties	20
(2-5-1)	Absorbance	21
(2-6)	Optical constants	22
(2-6-1)	Absorption coefficient	22
(2-6-2)	Refractive index and Extinction Coefficient	22
(2-7)	Fluorescence	23
(2-8)	Nanoparticles	27
(2-8-1)	Gold Nanoparticles (AuNPs)	27
(2-8-2)	Silver Nanoparticles (AgNPs)	28
(2-9)	Light Emitting Polymers (LEPs)	28
(2-10)	Laser Induced Fluorescence (LIF) Principle	30
(2-11)	Fluorescence Lifetime	32
Chapter three: Experimental Part and Materials		
(3-1)	Introduction	38
(3-2)	Materials used in this work	38
(3-2-1)	The MEH-PPV Polymer	38
(3-2-2)	The PFO Polymer	39
(3-2-3)	The Toluene	41
(3-3)	Experimental Work	43
(3-3-1)	Fabrication Technique of Samples: Laser	44

	Ablation in Liquids	
(3-4)	Samples Preparation	45
(3-4-1)	samples preparation of the MEH-PPV	46
(3-4-2)	samples preparation of the PFO	47
(3-4-3)	metallic nanoparticles preparation	
(3-4-4)	The Mixing of metallic nanoparticles with the LEP	47
(3-5)	Characterization Techniques of Samples	48
(3-5-1)	The Measurement of Absorption Spectra	48
(3-5-2)	Field Emission Scanning Electron Microscopy (FE-SEM)	48
(3-5-3)	The Measurement of Fluorescence Spectra	49
(3-5-4)	The Measurement of Laser-Induced Fluorescence Spectra	50
Chapter four: Results and Discussion		
(4-1)	Introduction	55
(4-2)	Eexperimental Results	55
(4-2-1)	Results FE-SEM Images	55
(4-2-2)	Results of the optical spectroscopy of the pure MEH-PPV polymer and the pure PFO polymer	56
(4-2-3)	Results of the optical spectroscopy of the Au NPs and the Ag NPs	58
(4-2-4)	Results of the optical spectroscopy of the matrixes (the Au NPs and the Ag NPs with LEPs)	59
(4-2-5)	Results of the fluorescence spectra of the matrix MEH-PPV with Au NPs	61
(4-2-6)	Results of the fluorescence spectra of the matrix PFO with the Ag NPs	63
(4-2-7)	Results of the laser-induced fluorescence of the matrix MEH-PPV with the Au NPs	65
(4-2-8)	Results of the laser-induced fluorescence of the matrix PFO with the Ag NPs	67
(4-2-9)	Results of the Time-life and Quantum Efficiency of Fluorescence of the LEP MEH-PPV	70
Chapter Five: Conclusions and Future Work		
(5-1)	Conclusions	77

(5-2)	Future studies	79
	References	

List of Figures

No. of figure	Subject	Page No
(2-1)	Surface resonance of metal nanoparticles	13
(2-2)	surface Plasmon polariton	13
(2-3)	Localized Surface Plasmon	14
(2-4)	Stokes shift between the absorption spectrum and emission spectrum	25
(2-5)	Jablonski Diagram	26
(2-6)	Optical devices used in LIF technology	31
(3-1)	The chemical structure of the MEH-PPV	39
(3-2)	The chemical structure of the PFO	41
(3-3)	The chemical structure of the toluene	42
(3-4)	The Scheme of the experimental work and the tests that are necessary to describe this work	43
(3-5)	Shows a scheme of the experimental setup used in NPs preparation by laser ablation confined in a liquid medium	44
(3-6)	The different concentrations of the MEH-PPV polymer	46
(3-7)	The different concentrations of the PFO polymer	46
(3-8)	The different concentrations of the matrix; a) the Au NPs with the MEH-PPV, and b) the Ag NPs with the PFO	47
(3-9)	The UV-Visible Spectrophotometer	48
(3-10)	Schematic of the FE-SEM device.	49
(3-11)	The Fluorescence Spectrophotometer	49
(3-12)	The LIF spectroscopy technique	50
(4-1)	The FE-SEM image of; a) the Au NPs, and b) the Ag NPs in the toluene solution	55
(4-2)	The Absorption spectra of a) the pure MEH_PPV in different concentrations, and b) the pure PFO in different concentrations	57

(4-3)	The absorption spectra of; a) the Au NPs in different laser pulses, and b) the Ag NPs in different laser pulses	58
(4-4)	The absorption spectrum of; a) the different concentrations of the MEH_PPV with the Au NPs, and b) the different concentrations of the PFO with the Ag NPs.	60
(4-5)	The fluorescence spectra of the MHE-PPV polymer with the Au NPs at different concentrations; a) $1 \cdot 10^{-4}$ M, b) $3 \cdot 10^{-4}$ M, and c) $5 \cdot 10^{-4}$ M	62
(4-6)	The fluorescence spectra of the PFO polymer with the Ag NPs at different concentrations; a) $1 \cdot 10^{-6}$ M, b) $3 \cdot 10^{-6}$ M, and c) $5 \cdot 10^{-6}$ M	64
(4-7)	The LIF spectra of the pure MEH-PPV polymer compared to the doped MEH-PPV polymer, of the wavelength-excited; a) 480 nm, and b) 532 nm.	66
(4-8)	The LIF spectra of the pure PFO polymer compared to the doped PFO polymer, of the wavelength-excited; a) 480 nm, and b) 532 nm.	69

List of Tables

No. of Tables	Subject	Page NO.
(3-1)	The physical and chemical properties of the MEH-PPV.	39
(3-2)	The physical and chemical properties of the PFO.	40
(3-3)	The physical and chemical properties of the toluene.	42
(4-1)	the wavelength shift with changing number of laser pulses.	70
(4-2)	the improvement in the quantum efficiency of the PFO after adding nanoparticles the Ag NPs at all concentrations.	71
(4-3)	the improvement in the quantum efficiency of the PFO after adding nanoparticles the Ag NPs at all concentrations.	

List of symbols

Symbol	Definition of symbol and term	Unit
α	linear Absorption coefficient	cm^{-1}
n	The linear refractive index	
k_0	Extinction Coefficient	
C	concentration	M
\vec{E}	Electric field intensity	V/m
\vec{H}	Magnetic field intensity	A/m
\vec{D}	Displacement current	I

\vec{B}	Magnetic induction	B
\vec{J}	Current intensity	A/m ²
ρ	Charge density	A.m ⁻³
\vec{P}	polarization	P
\vec{M}	Magnetism	H/m
σ	conductivity	S/m
ϵ_0	Vacuum tolerance	F/m
μ_0	Vacuum permeability	N/A ²
β	diffusion constant	M Per Sce
ω	Angular frequency	rad /sec
m_e	Free electron mass	Kg
X	Electron displacement	m
q_e	Electron charge	C
γ	Electronic damping factor	--
N	Number of electrons	—
Γ	Electronic damping ratio	--
R	The radius of the nanoparticles	nm
$\epsilon(\omega)$	Electrical insulation function of metal	--
σ_{acs}	Dispersion cross section	m ²

σ_{scs}	Absorption cross section	m^2
k	The wave vector of incident light	m^{-1}
v	Coupling coefficient	--
γ_p	The line width, or damping, corresponds to the minimum value associated with the plasmon.	--
γ_e	The line width, specifically the damping factor, represents the minimum value associated with the exciton.	--
w_m	The weight of the polymer needed to obtain the desired concentration	gm
$V_{1,2}$	The volume of solvent needed to be added to the substance	cm^3
M_w	Molecular weight of the polymer used	gm / mol
Φ_F	Fluorescence quantum yield	--
k_Q	Cooling process	--
K_{RET}	Resonance energy transfer	--
k_{IC}	Internal conversion	--
k_{ICS}	Crossing between systems	--
k_F	The number of photons emitted to the number of photons	--

	absorbed	
τ_{FM}	Radiative fluorescence lifetime	sec
K_F	The sum of the probabilities of radioactive and non-radiative transitions	-----
τ_f	fluorescence lifetime	sec
$I(t)$	fluorescence intensity at time t.	
I_0	initial fluorescence intensity at t = 0	
K_d	Non-radiological operations constant	-----
ϕ_f	Quantitative production of fluorescence	
$F(\nu')$	Fluorescence spectrum area	-----
$\epsilon(\nu')$	Absorption spectrum area	-----
S_n	The ground state of a molecule or atom	-----
S_1	Excited Singlet State	-----
S_0	Ground energy level	-----
$\tau_{polymer}$	Represents the chronological lifetime of the standard compound, which is the light-emitting polymer.	sec
$a_{polymer}$	It is the area under the fluorescence curve of the light-emitting polymer.	m

List of abbreviations

Symbol	Meaning
MEH-PPV	Poly[2-methoxy-5-(2-ethylhexyloxy)-1,4-phenylenevinylene]
PFO	Poly(9,9-di-n-octylfluorenyl-2,7-diyl)
LIF	Laser Induced Fluorescence
LEP _s	Light-emitting polymers
TADF	Thermally activated delayed fluorescence
UV-VIS	Ultraviolet–visible spectroscopy
TOTM	Tri-n-octylphosphine thiocyanate
PFOA	Perfluorooctanoic acid
SPR	Surface plasmon resonance
LED _s	light-emitting diodes
LSPR	localized surface Plasmon resonance
PEHF	(ethylene-co-hexamethylene 2,5-furandecarboxylate)
PEI	Polyethylene
OLED _s	organic light-emitting diodes
P3HT	poly(3-hexylthiophene)
PVA	Poly(vinyl alcohol)
RhB	Rhodamine B
Rh6G	Rhodamine 6G
PVP	Polyvinylpyrrolidone

LSP	localized surface Plasmon
SSP	Surface Plasmon polaritons
Nd-YAG	Neodymium-Doped yttrium Aluminum Garnet
CNT _s	Containing carbon NanoTubes
HTM	Hole Transporting Material
PMT	photomultiplier tube
Ag NP _s	Silver nanoparticles
Au NP _s	gold nanoparticles
FE-SEM	Field emission scanning electron microscopy
PLAL	Pulsed Laser-Ablation in Liquids
PLED	Polymer Light-Emitting Diodes

Chapter one

Introduction

1-1: Introduction

A Light-emitting polymers (LEPs) are a class of organic materials that are capable of emitting light. In the early 1960s, DuPont researchers discovered that certain organic materials could emit light under certain conditions, which led to the discovery of the LEPs. However, the first LEP was not effectively synthesized until the 1980s [1]. The LEPs, or light-emitting polymers, have grown in significance as a result of their special characteristics and possible uses. These benefits include environmental friendliness, energy efficiency, versatility, wide area coverage, and wavelength tenability. Numerous applications, including lighting, displays, sensors, and photovoltaics, are being investigated for the LEPs. Large sheets of them can be created, they can be tweaked to emit light in various hues, and they can be fashioned into flexible and bendable materials. They are also more ecologically beneficial than conventional lighting sources since they can be recycled [2].

The LEPs according to their chemical structures are classified physical properties. The most prevalent the LEPs are conjugated polymers, which consist of alternating single and double bonds. Phosphorescent polymers are light-emitting polymers (LEPs) that emit light for a longer duration than conventional fluorescent materials [3]. Ionic polymers are the LEPs that contain charged groups, such as quaternary ammonium compounds, and can emanate a broad spectrum of wavelength.

A Plasmons are collective oscillations of free electrons on metals and other conductive materials that are capable of interacting with light to produce unique optical phenomena. In the early 20th century, when scientists were investigating the optical properties of metals, so that plasmons were first studied [5].

The Plasmons are a promising technology with numerous potential applications in disciplines including biosensing, spectroscopy, photonics, and medicine. The Plasmons that occur at the point where a metal and a dielectric material meet, such as air or water, are known as Surface Plasmons Resonance (SPR). The SPR occurs in nanoparticles of metal or other structures with particular geometries. Bulk plasmons exist in the bulk of a metal or other conductor [6].

They can be stimulated by light or other means, including an electrical current. New plasmonic materials and structures with even more advanced properties and applications are the focus of ongoing research [7]. The effect of plasmons is related to the interaction of light with unbound electrons in metals and other conductive materials. When light interacts with metal nanoparticles or other nanostructures, it can excite plasmons, which can have numerous effects. One of the primary effects of plasmons is the enhancement of the electromagnetic field near the plasmonic nanostructure, which can be used to increase the sensitivity of various spectroscopic techniques [8]. The ability of plasmons to trap and manipulate light at the nanoscale is another effect of plasmons. Many nanomaterials, including metallic nanoparticles (such as gold or silver), graphene, and other two-dimensional materials can generate plasmons. The plasmonic properties of these substances depend on their size, shape and composition [9].

The Plasmon can have a significant impact on the optical properties of LEPs, depending on factors such as the type and size of the plasmonic structure, the optical properties of the LEPs, and the distance between the plasmonic structure and the LEP. The Plasmons can also reduce the intensity of fluorescence emission by quenching fluorescence emission [10]. The Plasmon can also result in LEPs degradation, as the enhanced electromagnetic field close to the plasmonic structure can generate reactive species that can degrade the polymer.

Plasmons can also modify the LEPs absorption and emission spectra, resulting in color and luminance changes. Excitons are electron-hole pairs formed when a light-emitting polymer absorbs a photon and can degrade either radiatively or nonradiatively. Researchers are actively examining the plasmon- exciton interaction in order to create new plasmon-enhanced optical devices and sensors with enhanced sensitivity, color purity, and resolution [11].

Coupling between a plasmon generated by nanoparticles and an exciton generated by LEPs is a complex phenomenon that can have a substantial effect on the optical properties of the system [12]. The Plasmon on the other hand, are the collective oscillations of unbound electrons within a nanoparticle metal. Long-range interactions can facilitate coupling between the nanoparticle and the LEPs [13]. This coupling can result in a number of fascinating optical phenomena, including the enhancement or suppression of fluorescence, the modification of the emission spectrum of the LEPs, and the modification of the plasmonic resonance frequency. These effects have significant implications for the design of plasmon-enhanced optoelectronic devices such as solar cells, light sources, and sensors [14]. The focus of research is on developing new materials and enhancing their properties for diverse applications [4].

1-2 Literature review

In 2010, Paulo B. Miranda et al. [15], studied the photoluminescence properties of MEH-PPV, a kind of PPV-based polymer, under UV excitation. They found that the photoluminescence efficiency decreases for excitation energies between 2.1 and 2.5 eV, but is higher for energies below the absorption maximum. These results indicate that the states excited in UV light relax non-radiatively rapidly to the lowest state. The authors also note that typical photoluminescence is only detected during UV photocatalysis, and that the emission properties are affected by morphology, excitation energy, and temperature. The study indicates that spectral overlap in the MEH-PPV induces energy transfer and interband shifts, leading to rapid excited-state energy relaxation and non-radiative decay channels. These results have implications for the performance of polymer-based conjugated optoelectronic devices.

In 2013, Gao et al. [16], studied the effect of silver nanoparticles on the emission of poly(9,9-dioctylfluorenyl-2,7-diyl) (PFO). The authors observed an increase in the intensity of the PFO emission when silver particles were present in the system. This enhancement is attributed to the localized surface Plasmon resonance (LSPR) effect exhibited by the silver nanoparticles.

In 2012, Mucur et al. [17], investigated the influence of silver (Ag) conductor and titanium dioxide (TiO₂) semiconductor nanoparticles on polymer organic light-emitting diodes (P-OLEDs). Composite layers, incorporating these nanoparticles into the hole transport layer (PEDOT:PSS) and the emissive layer (MEH-PPV), were fabricated using solution processing. The resulting P-OLEDs exhibited improved efficiency (up to 45%) when incorporating Ag nanoparticles, with TiO₂ nanoparticles enhancing threshold and turn-on voltages. The electroluminescent spectrum was minimally affected by Ag nanoparticles but shifted to shorter wavelengths with TiO₂. Inserting TiO₂ into

the hole transport and MEH-PPV layers enhanced device performance, including a 38% increase in luminance. Both semiconductor and conductor nanoparticles facilitated more efficient charge injection, transport, and recombination. However, further research is needed to explore device stability and lifetime.

In 2015, Xiaoyan et al. [18], investigated the impact of strategically incorporating gold nanoparticles into polymer light-emitting diodes (PLEDs) to enhance efficiency. By leveraging the unique "far-field" effect of gold nanoparticles, the research aims to optimize light emission and overall device performance. The findings suggest that the intentional integration of these nanomaterials holds great promise for advancing PLED efficiency in optoelectronic devices. The study concludes by summarizing key discoveries and outlining potential implications for the field, highlighting the significance of utilizing gold nanoparticles with distinct optical properties for future advancements in PLED technology.

In 2016, T.H.T. Aziz et al. [19], The study investigated the impact of surface grinding on Ag nanosheets on the electroluminescent properties of Ag polymer light-emitting diodes. The diodes featured a Poly (ethylene-co-hexamethylene 2,5-furandecarboxylate) (PEHF) layer as the photo-emitting device, incorporating 5 wt% Ag nanosheets. Results revealed a significant 51.85% increase in electroluminescence intensity compared to devices lacking Ag nanosheets. This enhancement was attributed to the interaction between surface Ag ionophores and light emitted by PEHF. The conjugation process was validated by the shorter PEHF:Ag layer lifetime, measured through time-resolved photoluminescence spectroscopy. Additionally, the overlap between the photoluminescence peak of PEHF at 425 nm and the absorption peak of

surface Ag nanosheets was demonstrated. Overall, the study highlighted that integrating Ag nanosheets into the diode's photodiode layer could boost electroluminescence brightness through the coupling of Ag surface Plasmon and light emitted from the PEHF polymer.

In 2017 ,Yingjie Zhang et al. [20], studied the performance and operational stability of polyethylene (PEI)-based electron injection layers used in solution-cured organic light-emitting diodes (OLEDs). The cathode metal used in contact with the EIL determines the main mechanism of degradation in these OLEDs. The operational life of OLEDs can be increased to more than 1000 hours without device performance degradation by using a mixture of PEI and ZnO nanoparticles as EIL to significantly reduce the emitter/PEI/Al interface degradation by excitons. The results of this work show that efficient and reliable OLEDs can be produced using electron injection materials that have undergone solution processing.

In 2019 ,Ruizhi Wang et al. [21], studied the optical properties of poly[2-methoxy-5-(2-ethylhexyloxy) -1,4-phenylenevinylene] (MEH-PPV) films using absorption and photoluminescence spectra at different temperatures below 200 K. Interchain coupling was stronger in the films generated from the chlorobenzene solution compared to those from the chloroform solution. Annealing the MEH-PPV films at 420 K and 520 K significantly increased the coupling between the chains, resulting in an H-complex-like behavior that dominates the PL properties. The research confirmed that the HJ aggregate model can be applied to describe the photophysical properties of cross-linked polymer films using adjustable interchain coupling.

In 2022 , Tooba et al. [22], studied the interaction between silver nanoparticles' surface plasmon resonance (SPR) and poly(9,9-dioctylfluorenyl-2,7-diyl) (PFO)

emission properties. They found that the SPR of silver nanoparticles can enhance PFO's emission intensity and quantum yield. The study found that when silver nanoparticles were incorporated, their SPR could interact with PFO's emission properties, resulting in an enhancement of PFO's emission intensity and quantum yield. This interaction played a crucial role in improving PFO's emission properties.

In 2019, politesi.polimi.it et al. [23], studied the surface interactions between the semiconducting poly(3-hexylthiophene) (P3HT) polymer and the electrolyte solution. They used plasmonics to characterize this interface but ran into limitations due to the hydrophobic nature of the polymer, which prevented the solution from penetrating into the block. Despite this, they observed a resonance enhancement of polymer absorption and suggested potential applications in improving implant performance and providing optical filtration. They proposed alternative methods such as the deposition of gold nanoparticles on the polymer surface or increasing the porosity of the film to improve the local pH resolution. The study emphasized the potential of plasmonics in enhancing polymer adsorption and called for further research to overcome challenges and refine characterization techniques.

In 2020, Kesavan et al. [24], Study confirming the formation of complex nanoparticles of poly(2-methoxy-5-(2-ethylhexyloxy)-b-phenylphenylene) NP adsorbed with Au NPs by high-resolution electron microscopy and infrared Fourier experiments. The photoluminescence (PL) efficiency of laser microscopy of the complex increased significantly compared to that of single MEH-PPV NP without Au NPs, which was directly confirmed by images of the color charge-coupled device. The improved PL efficiency may have arisen from the energy transfer effect of surface plasmon resonance coupling and/or the strong local field enhancement at the nanoscale.

In 2021, N. S. Shnan et al. [25], studied the optical properties of polymer solutions with different concentrations of rhodamine dye with the aim of creating an efficient waveguide. Polyvinyl pyrrolidone (PVP) and polyvinyl alcohol (PVA) polymers in different ratios were used to create a three-layer waveguide, the central layer of which has a greater refractive index than the upper and lower layers. The best laser emission performance was demonstrated by the PVA + RhB (10-4M) model, while the highest signal transmission performance was demonstrated by the PVA + Rh6G (10-5M) model. In addition, the surface plasmon resonance (SPR) effect generated by silver nanoparticles (Ag NPs) in the samples altered the pumping threshold and improved the waveguide effectiveness. The fluorescence and absorption spectra of the polymer dye solutions were shown.

In 2021 ,N.S. Shnan et al. [26], Used a laser to study surface Plasmon resonance (SPR) on nanomaterials (gold and silver). Four samples of varying composition were illuminated with two lasers: a green laser (532 nm) and a blue laser. Its wavelength is (402 nm), and the findings showed that the green laser produced the greatest SPR irritation for the gold sample, while the blue laser produced the best SPR irritation for the silver sample. The blue piezo laser is employed, and as its power increases, the interaction between the rise in energy and the increase in concentration occurs.

In 2021 , Zhao et al. [27], studied the coupling between gold nanoparticle erosion and photoluminescence in organic polymers with different doping concentrations. They found that gold nanoparticles with different doping concentrations can enhance the emission intensity of organic polymers. The study aimed to explore the interaction between the occlusivity of gold nanoparticles and photoluminescence, revealing that the extent of improvement differed with different doping concentrations of gold nanoparticles

1-3 Aim of the Work and Research Motivation

The current study aimed to improve the optical properties of two types of light-emitting polymers (MEH-PPV and PFO). This improvement in properties depends on adding metal nanoparticles (Au NPs, and Ag NPs) at different concentrations to the light-emitting polymers. The optical properties of the LEPs are improved by taking advantage of the phenomenon the coupling between the Plasmon generated from the nanomaterials and the exciton generated from the light-emitting polymers.

Chapter Two

Theoretical part

2-1 Introduction

This chapter describes the basic concepts, theories and physical phenomena of light-emitting polymers as well as of metal nanoparticles and their generation. It also describes the optical properties of light-emitting polymers and the importance of improving them.

2-2 Surface Plasmon Resonance (SPR)

A Surface Plasmon resonance (SPR) is a physical phenomenon that occurs when polarized light interacts with a thin metal film (near or on surface) this property appears clearly in gold, silver, and copper in the visible light region and is responsible for the change of color when these elements reach the size of the nanoparticles. The photons are transferred to the free electrons on the surface of the metal, causing them to oscillate collectively. This collective oscillation of electrons is called a surface Plasmon [28,29]. The SPR has many applications in physics and engineering, including biosensing, surface-enhanced spectroscopy, and nanophotonics. It is used to detect biomolecular interactions, enhance signals from Raman scattering, fluorescence, and other spectroscopic techniques, and manipulate and control light at the nanoscale, enabling new applications in optical communication, sensing, and imaging [30,31]. Plasmon nanostructures are a major part of nanophotonics that can trap electromagnetic waves smaller than the diffraction limit, and nanofabrication techniques are helping to increase their applications [32]. When electromagnetic waves fall on a metal surface, they will accelerate electrons and cause polarization which results in a restoring force that causes the metal's free electron to oscillate as shown in the Figure (2-1). This fluctuation is quantized and the fluctuation of free electrons is a quantization of plasma fluctuations and is called a surface Plasmon Resonance [33]. Depending on the shape, there are two types of surface plasmons: surface Plasmon polaritons (SPP) and localized surface Plasmon (LSP).

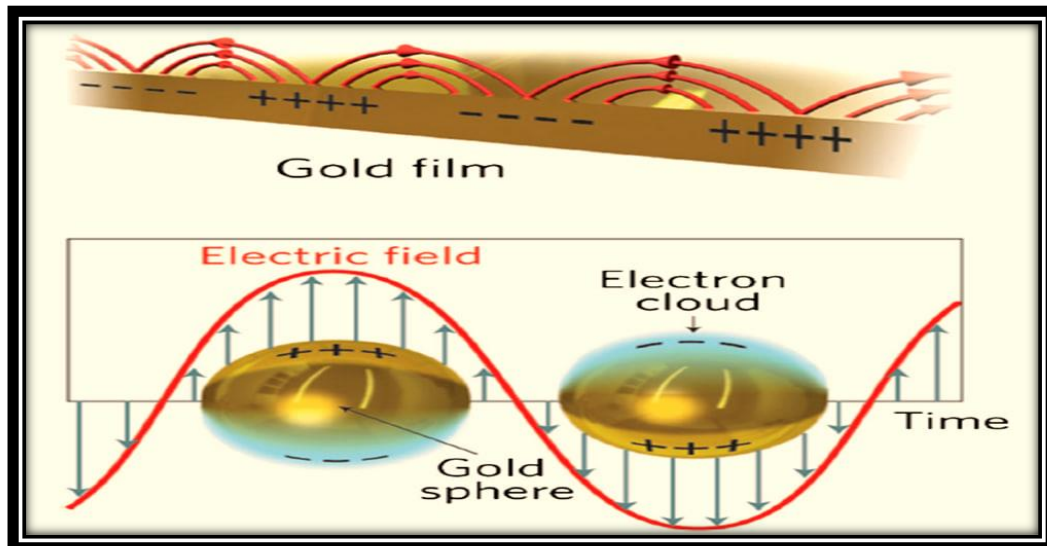


Fig (2-1): Surface resonance of metal nanoparticles [34]

2-2-1 A Surface Plasmon Polariton (SPP)

Surface Plasmon Polariton (SPP) is a collective oscillation of electrons at the interface between a metal and a dielectric (insulator) material. It typically occurs at optical frequencies. This phenomenon is a result of the coupling between electromagnetic waves and the free electrons on the metal surface. [35].

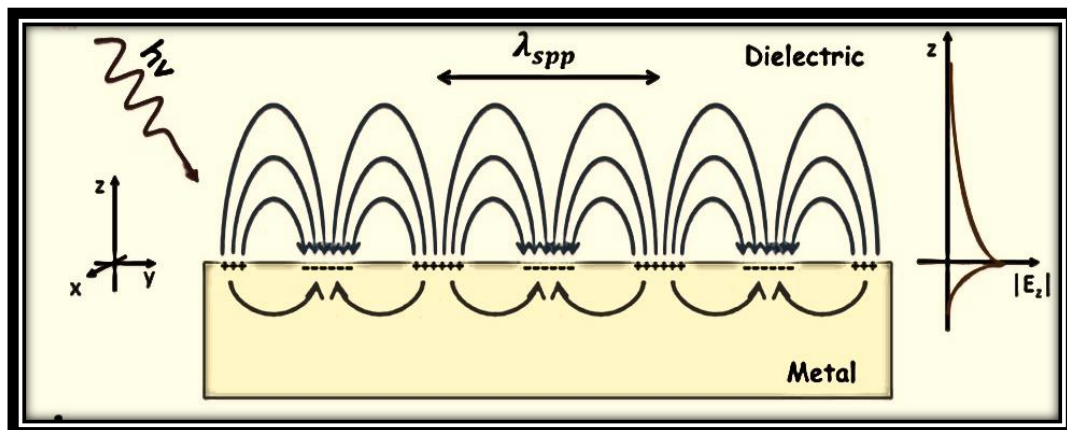


Fig (2-2): surface Plasmon polariton [36]

2-2-2 A Localized Surface Plasmon (LSP)

The LSP is a phenomenon in physics that occurs when a localized electromagnetic field is generated around metallic nanoparticles due to the collective oscillation of their conduction electrons in response to an incident electromagnetic wave [152]. The interaction between the incident electromagnetic wave and the metallic nanoparticle is described by the Plasmon resonance condition, which is determined by the size, shape, and composition of the nanoparticle. Applications of LSP include the study of plasmonics, the interaction of light with matter at the nanoscale, and the development of new materials with unique optical properties. It also has potential applications in energy harvesting, optical communication, and information storage [37].

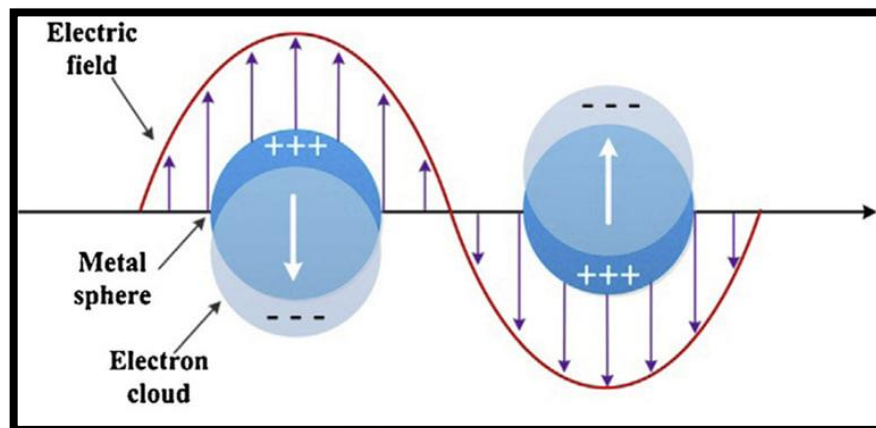


Fig (2-3): Localized Surface Plasmon [38]

Surface Plasmon Resonance (SPR) is the interaction of electromagnetic fields with metallic nanostructures, elucidated through the application of Maxwell's equations. Maxwell's equations for the electromagnetic field of a given system describe the categories involved 1- Electric field strength (E) 2- Electric displacement (D) 3- Magnetic field (H) 4- Magnetic motive (B) [39].

$$\nabla \cdot \vec{E} = \frac{\rho_e}{\epsilon_0} \quad \dots \dots \dots (2 - 1)$$

$$\nabla \cdot \vec{B} = 0 \quad \dots \dots \dots (2 - 2)$$

$$\nabla \times \vec{E} = -\frac{\partial \vec{B}}{\partial t} \quad \dots \dots \dots (2 - 3)$$

$$\nabla \times \vec{B} = \mu_0 \epsilon_0 \nabla \times \frac{\partial \vec{E}}{\partial t} + \mu_0 \vec{J} \quad \dots \dots \dots (2 - 4)$$

(μ_0) (ϵ_0): Permeability and Permittivity of free space.

ρ_e : total charge density.

\vec{J} : is the total current density.

The incident external electric field excites the free electrons and drives them away from their normal positions in the metal lattice. The motion of free oscillating electrons can be described by the equation of motion [40].

$$m_e \ddot{x} + m_e \gamma \dot{x} = -q_e E \quad \dots \dots \dots (2 - 5)$$

Where

m_e : free electron mass.

x : the displacement of the electron.

q_e : the charge of an electron.

E : is the external electric field.

γ : electronic damping factor.

The solution to equation (2-5) for a given amplitude (x_0) is the general solution for the oscillating electric field $E = E_0 e^{-i\omega t}$ [41].

$$x_0 = \frac{q_e}{m_e(\omega^2 + i\omega\gamma)} \epsilon_0 \quad \dots \dots \dots (2 - 6)$$

(ω) : is the angular frequency.

The height of the polarization electron microscope is $P = -Nq_0 x$ in the case of (N) is the number of electrons and is given by:

$$P = \frac{Nq_e^2}{m_e(\omega^2 + i\omega\gamma)} E \quad \dots \dots \dots (2 - 7)$$

The electrical displacement (D) depends on the dielectric function of the free electron as follows:

$$D = \epsilon_0 E + P \quad \dots \dots \dots (2 - 8)$$

Equation (8) becomes:

$$D = \epsilon_0 \left(1 - \frac{\omega_p^2}{\omega^2 + i\omega\gamma} \right) E \quad \dots \dots \dots (2 - 9)$$

Plasma frequency for free electrons [49].

$$\omega_p^2 = \frac{n q_e^2}{\epsilon_0 m_e} \quad \dots \dots \dots (2 - 10)$$

ϵ_ω The dielectric permittivity of the free electron is

$$\epsilon_\omega = 1 - \frac{\omega_p^2}{\omega^2 + i\omega\gamma} \quad \dots \dots \dots (2 - 11)$$

This equation describes the plasmonic behavior of a bulk metal using the Drude model.

So that a very small spherical metal nanoparticles when compared to the wavelength of the incident light, the polarizability of the nanoparticles (P_a) is

$$P_a = 4\pi R^3 \frac{\epsilon(\omega) - \epsilon_d}{\epsilon(\omega) + 2\epsilon_d} \quad \dots \dots \dots (2 - 12)$$

where

(R): the radius of the nanoparticles.

$\epsilon(\omega)$: the electrical permittivity of the metal.

ϵ_d : permittivity of the medium.

The optical cross-section of spherical nanoparticles enhances their strong scattering and absorption properties under Plasmon conditions and is given by [42].

$$\sigma_{\text{scs}} = \frac{k^4}{6\pi} |\text{Pa}|^2 \dots \dots \dots (2 - 13)$$

$$\sigma_{\text{acs}} = \text{klm} [\text{pa}] \dots \dots \dots (2 - 14)$$

$(\sigma_{\text{scs}})(\sigma_{\text{acs}})$: are the scattering and absorption cross sections.

(k) : is the wave vector of the incident light [43].

2-3 Excitons.

Excitons are quasiparticles that are created when an electron and a hole collide in a substance like an insulator or semiconductor. A hole is left behind in the lower energy state when an electron is stimulated to a higher energy state by taking in a photon. An exciton may then be created via the Coulomb interaction between the electron and hole. Excitons are not genuine particles, yet they behave like particles with their own energy and motion. Unlike individual electrons and holes, they may travel through the material and interact with light in numerous ways. Excitons are of special relevance in the creation of optoelectronic devices, such as solar cells, light-emitting diodes, and photodetectors, and have been widely investigated in the area of condensed matter physics. Excitons in semiconductors may either be bound or unbound. Unbound excitons may dissociate more readily and have a shorter lifespan than bound excitons, which are more tightly bonded and have a longer lifetime. Many variables, including the characteristics of the material, temperature, and external electric or magnetic fields, may influence the behavior of excitons. In general, the study of excitons is a significant area of physics research, having potential applications in a variety of areas such as optoelectronics, photonics, and energy conversion. For the creation of novel materials and systems that may

Make use of exactions' distinct qualities, it is crucial to comprehend their characteristics and behavior [44,45].

2-4 -Plasmon -Exciton Coupling

Exciton-plasmon coupling is a process that results in improved light-matter interactions and unique optical characteristics when excitons and Plasmon combine [46]. In a metal, Plasmon is a group of oscillating electrons that may be energized by the incoming light. Strong interactions and novel optical characteristics may result from the coupling of Plasmon and excitons in semiconductors [47]. The electromagnetic field interacts with both kinds of particles to cause the coupling of excitons and Plasmon [48]. Excitons and plasmons are capable of exchanging energy, enhancing light absorption and emission. Exciton-plasmon polaritons, which possess hybrid features shared by excitons and plasmons, are only one example of the novel quasiparticles that might result from this interaction [49]. In the realm of nanophotonics, where it has the potential to be used in the creation of novel kinds of optoelectronic devices, including photodetectors, solar cells, and light-emitting diodes, exciton-plasmon coupling has been intensively explored. Controlling the nanomaterials size, shape, and composition as well as adjusting the plasmon resonance frequency may improve coupling. The exciton-plasmon coupling is a fascinating area of physics study with potential applications in a variety of areas, such as nanophotonics, energy conversion, and information technology. It offers a new method for regulating and modifying light-matter interactions at the nanoscale and has the potential to create new gadgets that perform better and have more features [50]. Strong coupling may be achieved thanks to the heightened electromagnetic fields of the excitons powerful oscillators. Since the intrinsic properties of SPP and exciton modes are unaltered in the surface plasmon-exciton weak coupling domain, the particle absorption or emission

rates rise [51]. Nevertheless, the SPP and exciton modes are altered by the production of new linked modes when the coupling is thought to be significant, leading to an anti-crossing behavior in the scattering curve [52]. When the surface plasmon and exciton modes resonate at the same frequency, anti-crossing is seen. As shown theoretically and empirically, two newly created energy states are divided by an energy value known as the energy difference that possesses a Rabi splitting energy in a strong plasmon-exciton coupling regime. Energy for splitting the Rabi is provided by [53].

$$\hbar_R = \sqrt{4V - (Y_p - Y_e)^2} \quad \dots \dots \dots (2 - 15)$$

where

(V) is the coupling coefficient

(Y_p)(Y_e) the linewidths (i.e., damping) of the Plasmon minimum , respectively.

The degree of this interaction effectively controls the optical characteristics of a hybrid system like this one affecting the absorption and emission characteristics of molecules positioned near to the plasmonic structures [54].

The Split can be set in two ways:

1- By altering a material, such as a component, excitonic characteristics (y_e or V)

2. By adjusting the plasmonic system properties (any change Y ρ)

In the strong coupling regime, surface plasmon damping has recently been used to tune surface plasmon-exciton coupling and subsequently Rabi decoupling energy [55]. Plasmon and exciton coupling are significant physics phenomena, especially in the research of light-emitting polymers [56]. Plasmon coupling is the connection between plasmons, which are the collective oscillations of electrons in a metal, and excitons, which are the excited states of a molecule. In the context of light-emitting polymers, this coupling increases the efficiency of

energy transfer from plasmons to excitons , hence enhancing light emission [57]. Contrarily, exciton coupling refers to the interaction between excitons in nearby molecules. This may result in a phenomena known as exciton delocalization, in which the excitons are dispersed across a greater region and can interact with more plasmons as a result. This may also increase the polymers light emission [58]. The coupling between plasmons and excitons is very reliant on the materials physical structure, such as the size and form of the metal nanoparticles and their distance from the polymer molecules. For the development of effective light-emitting polymers and other optoelectronic devices, it is vital to understand and regulate these interactions [59].

2-5 Linear Optical Properties

The optical characteristics of materials result from the interaction between the kind and distribution of charges inside the material (electronic, molecular, or ionic) and electromagnetic radiation [60]. When electromagnetic radiation falls on a material and interacts with it, many processes occur as a portion of the electromagnetic radiation is absorbed by the material, another portion is called the transmitted ray because it passes through the material, and a final portion is called the reflected part because it is reflected from the surface of the material [61]. To obtain information about interference, the materials composition, and the nature of its bonds, it is necessary to measure the, reflectivity absorption, and transmittance of electromagnetic radiation incident on the material. For instance, the ultraviolet spectrum identifies the energy packets and quality of transitions inside a material, while the visible spectrum identifies the range of practical applications in which the material is used [62].

2-5-1 Absorbance.

It is the process by which radiation transfers some or all of its energy to the material through which it passes or the process of decreasing the intensity of certain frequencies (certain wavelengths) of electromagnetic radiation. In the

case of Liquid materials: The probability of the solution absorbing incident photons is directly proportional to the concentration of molecules absorbed into the sample. The mathematical expression between the density of molecules (concentration) in the sample and the thickness of the sample The incident ray passes through it (optical path length) is the absorbance or optical density [63,64].

$$A = \text{Log} (I_0/I) \quad (2.16)$$

where: I_0 : intensity of incident ray, I : intensity of the transmitted ray through the sample.

The energy transfer from the incident electromagnetic wave to the material passing through happens by the electric field of the incident photon interacts with the momentum of the electric dipole of the material. This leads to the electron a rise to a higher energy level, so decrease the incident intensity [65,66].

$$I = I_0 e^{-\epsilon cl} \quad (2.17)$$

When the incident energy sufficient to cause an electronic transition in the matter, the absorbance increase with increases the concentration of the molecules that absorb the electromagnetic wave According to Beer Lambert's law "For a given material, the sample path length and concentration of the sample is directly proportional to the absorbance of the light." The Beer lambert law applied if the "light monochromatic" [67,68].

$$A = \epsilon cl \quad (2.18)$$

where: ϵ molar extinction coefficient (molar absorptivity) $M^{-1} \text{ cm}^{-1}$, C molar concentration of the absorber substance in (M), l optical length.

2-6 Optical constants

2-6-1 Absorption coefficient (α)

The absorption coefficient is an important optical factors, which represent how far light penetrate before absorbed by the material. The Absorption coefficient depends on the photon energy and properties of the material under study. The absorption coefficient can be determined from the optical absorption spectrum by the following equation [69].

$$\alpha = 2.303 \frac{A_0}{t} \quad (2.19)$$

where, t is the sample thickness and A_0 is defined by $\log(I_0/I_a)$ where I_0 and I_a are the incident intensity and transmitted intensity beams, respectively.

2-6-2 Refractive Index and Extinction Coefficient

The Refractive Index (n) is the ratio between the velocity of light in vacuum (c) to the velocity of the light in medium (v), $n = c/v$. The refractive index of a specific material exhibits wavelength dependence for incident electromagnetic waves. With certain materials, the refractive index not only varies with wavelength but also changes based on the direction of the electromagnetic waves within the material. Consequently, these materials can alter the polarization direction of the waves. The complex refractive index is mathematically represented by the following equation [70,71]:-

$$\bar{n} = n + i \kappa \quad (2.20)$$

where, n : the real part (the usual) of complex refractive index, κ : extinction coefficient which is the imaginary part of the complex refractive index, both depend on frequency (ν).

$$\kappa = \alpha\lambda/4\pi \quad (2.21)$$

When an electromagnetic wave at a certain frequency falls on a material it works to change the position of the material charge from its original position producing a dipole. So the electrical polarization of the molecule will oscillate with the frequency of the electromagnetic wave, this will transfer part of the energy of the incident wave to oscillating energy for the generated electric dipole, this will reduce the amplitude of the incident wave [72].

There is a relation between the refractive index and the polarization caused by the electromagnetic wave, when refractive index increase leads to decrease the speed of the light inside matter, the delay effect increases. However, when the value of the refractive index is equal to one that means there is no delay and there is no polarization [73,74].

2-7 Fluorescence.

When a material absorbs electromagnetic radiation, it becomes excited and gains energy as a result. This irritant may emit photons with various energy until it achieves a steady state. In other words, when those particles return to their initial level of energy (S_0), they will release photons with the same energy and wavelength. In certain cases, a radiating system can absorb a significant amount of energy, causing some electrons to be excited to energy levels beyond the stability threshold of the molecule. Subsequently, the system may promptly return to its initial state. to its stable state by producing photons with the same energy as the absorbed photons. The absorbed electrons may also return to the ground state by emitting photons with low energy, i.e., less energy and a longer wavelength than the photons they have absorbed. The term for this phenomena is fluorescence [75, 76]. Fluorescence is a spontaneous emission phenomenon. It takes place between two levels with the same multiplicity [78]. During the absorption process, the molecules spend a very brief amount of time ranging from (10^{-6} - 10^{-9}) seconds at the excited level, which is referred to as the lifetime of the dye molecules. When particles return to the by producing photons,

fluorescence may take place [79]. At room temperature, the molecules are in the lowest vibrational level of the ground level. As a result, absorption occurs from the zero vibrational level of the ground level to one of the levels of the excited , in which case fluorescence can occur as a result of the molecules undergoing transitions.

Fluorescence photons are emitted by the electronic transitions depending on the nature of the particles. It occurs in liquids and thick media and is known as normal fluorescence [80]. The alteration in vibrational levels during the transition from the excited state to the occurrence of normal fluorescence is referred to as vibrational relaxation. This process occurs within a specific time period, typically ranging from 10^{-13} to 10^{-11} seconds. Relaxation leads to vibration increases the temperature of the sample and causes the emission spectrum (fluorescence) to shift in length the long wavelength is called the (Stoke's shift) [81]. Stoke's offset is the shift that indicates lower energy between incident light and diffused or emitted light after interaction with the sample. The wavelength of these lines is longer than the wavelength of the excited radiation responsible for the absorption of the process [82]. The Stokes offset can be defined as the difference in wavelength or frequency units in the position of the spectra absorption and emission (fluorescence) for the same electron transitions. Stokes displacement occurs due to relaxation vibratory at agitated levels [83]. Figure (2-4) below shows the relationship between the absorption spectrum and the emission spectrum.

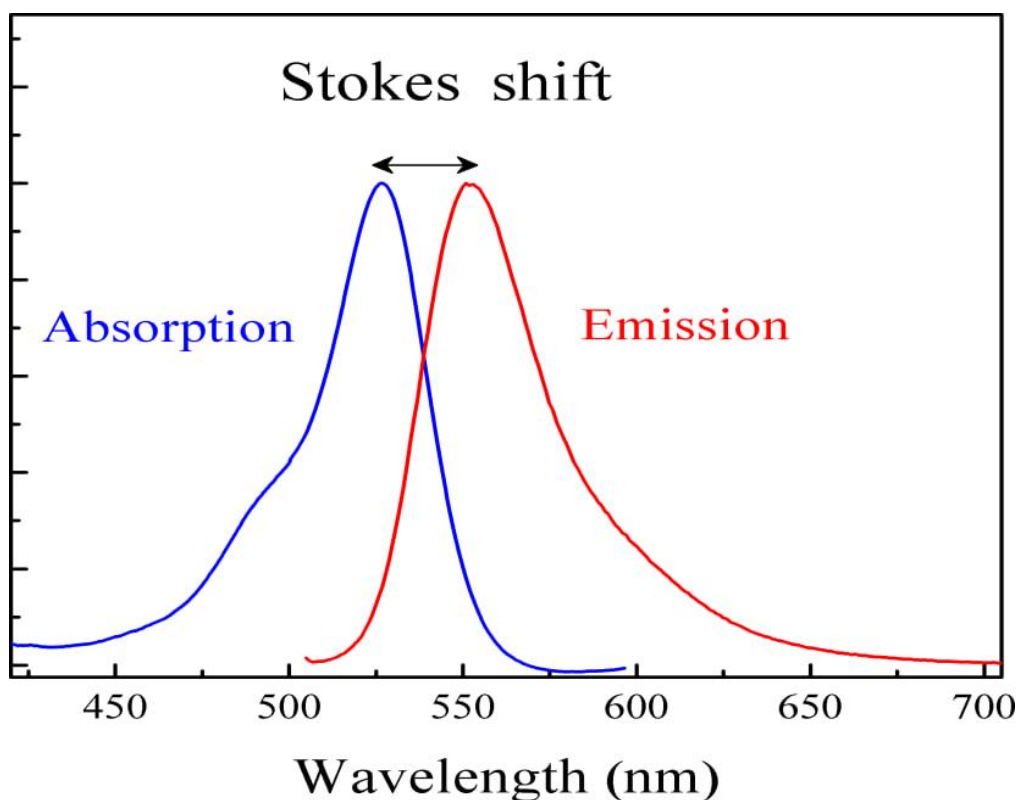


Fig (2-4): Stokes shift between the absorption spectrum and emission spectrum (fluorescence) [84].

Figure (2-5) A Jablonski energy diagram is used to describe the most important processes visual physical. Absorbed light excites particles of matter from their lowest levels of the ground state (S_{00}) to higher vibrational levels of state (S_{1n}) and thermal redistribution of the groups between the chains sublevels within a very short period of time (10^{-11} sec) [88]. It uses a Jablonski energy diagram to explain how organic molecules, called light-emitting polymers behave when they are activated by an electric current or another kind of energy [89].

In the Jablonski energy diagram, energy levels are represented by horizontal lines, with greater levels of energy situated above lesser ones. Typically, the graphic depicts the ground state of the molecule or substance, as well as the many excited states that may be reached as energy is absorbed. The excited states may have a brief lifetime, reverting to the ground state by non-radiative processes, or they may decay to lower energy levels by producing light [90].

The Jablonski diagram for light-emitting polymers generally contains the lowest excited singlet state (S_1), which is responsible for light emission. This condition may be achieved by absorbing energy from an external source, such as an electric current. The excited state may return to the ground state by a variety of mechanisms, including non-radiative relaxation and light emission. The energy of the light released corresponds to the energy gap between the S_1 and ground states [92]. The Jablonski energy diagram offers an overall framework for understanding the behavior of light-emitting polymers and other light-emitting materials. It aids in illuminating the complicated energy transitions that occur during excitation and emission and may be used to enhance the performance of these materials in a variety of applications [93].

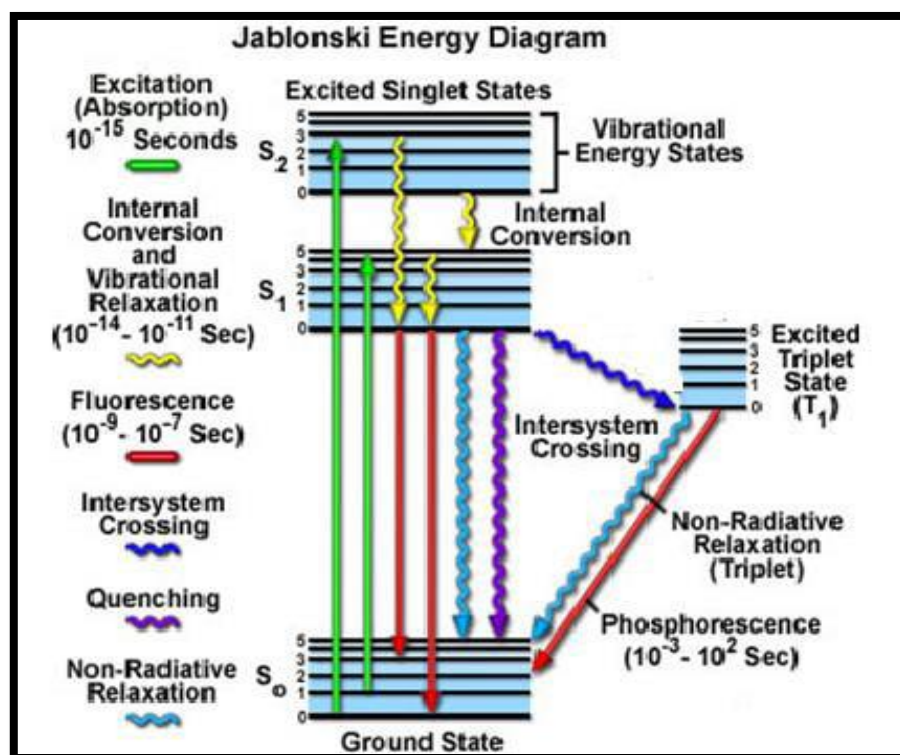


Fig (2-5): Jablonski Diagram [94].

2-8 Nanoparticles.

The nanoparticles are the most basic type of structure. In theory, a nanoparticle can be any group of atoms that are bound together and have a structural radius of less than 100 nm. Nanoparticles are now employed in numerous dosage forms because of their high solubility, small size, and improved penetration [95]. They can be made from a variety of materials, including metals, semiconductors, ceramics, polymers, and composites. Nanoparticles can have a higher surface area-to-volume ratio, different optical, electrical, magnetic, and chemical properties, and can exhibit unique behavior due to their size, shape, and surface chemistry. Nanoparticles have many potential applications in the different fields such as medicine, electronics, energy, and materials science. They are being developed for use in drug delivery systems, imaging agents, sensors, catalysts, and electronic devices, among other things. However, their small size and unique properties can also pose potential risks, such as toxicity and environmental impact, which must be carefully studied and managed [96,97]. Nanoparticles have a greater improvement in chemical and physical properties compared to bulk materials due to their very large surface area to volume ratio. The properties of nanoparticles (physical and chemical properties) depend on the structure, physical stability, size, shape and distribution of nanoparticles, which are examined using different microscopic techniques such as transmission electron microscopy and scanning electron microscopy [98,99].

2-8-1 Silver Nanoparticles (AgNPs)

The Silver (Ag) nanostructures have gained significant interest in various fields due to their unique properties, which are highly dependent on their composition, size, and shape [100,101]. Controlling these properties allows for the examination of electrical and optical properties and can be enhanced by manipulating their shape. Ag has the highest thermal and electrical conductivity

among metals and exceptional optical properties, making it a popular choice in photography [102]. Nano silver offers stability at ambient conditions, a lower cost compared to other noble metals like gold and platinum, a broad absorption band in the visible electromagnetic spectrum, chemical stability, and nonlinear optical behaviour. Surface Plasmon resonance, the collective oscillation of conducting electrons when excited by light at specific wavelengths, enables silver nanomaterials to interact powerfully with light. The maximal resonance wavelength of silver nanomaterials can vary between 380 and 470) nm based on their size and shape [103].

2-8-2 Gold Nanoparticles (AuNPs).

Gold nanoparticles are distinguished by their tiny size and composition, which has led to intense physics research into their plasmonic properties. By enabling free electrons to fluctuate in reaction to light, gold nanoparticles exhibit localised surface plasmon resonance (LSPR), which improves interactions between light and matter. They are excellent for a variety of applications in nanophotonics, sensing, and catalysis due to their adaptable plasmonic properties that can be changed by altering size, shape, and environment. Due to their powerful light scattering properties, gold nanoparticles are helpful in plasmonic metamaterials, bioimaging, and medicinal applications. They are a vital research tool in fields including nanophotonics, materials science, and biotechnology due to their distinctive plasmonic properties. Depending on size and form, the maximum resonance wavelength of gold nanoparticles may range between 500 and 600) nm [104,105].

2-9 Light Emitting Polymers

A Light Emitting Polymers (LEPs) are a category of organic polymers that emit light when subjected to an electrical current or other types of energy. They consist of conjugated organic molecules or polymers with delocalized electrons capable of absorbing and emitting light [106]. Because to the fact that LEPs

have the potential to be used in a variety of applications such as lighting, displays, and sensors, they have drawn considerable interest in physics and materials science. LEPs' versatility which enables easy shaping and integration into a range of devices, is one of its main advantages. They are appealing for large-scale applications since they are inexpensive and lightweight [107]. The absorption spectrum and emission spectra of light-emitting polymers (LEPs) are essential features that explain these materials' capacity to absorb and emit light [108].

The absorption spectrum of a Medium denotes the spectrum of light wavelengths that may be absorbed by the material. As light is absorbed by a conjugated polymer, the electrons are driven to higher energy levels, producing excitons that produce light. [109,110].

The emission spectrum of a substance defines the range of light wavelengths that the material emits. As decay light-based energy is released. The emitted light's energy is proportional to the energy bandgap of the LEP and the energy levels of the excited states participating in the decay process. Spectroscopy methods such as photoluminescence spectroscopy are commonly used to measure the emission spectrum [111,112].

The energy difference between the highest occupied molecular orbital (HOMO) and the lowest unoccupied molecular orbital (LUMO) determines the wavelength of the emitted light and is connected to the absorption and emission spectra of LEPs. By manipulating the energy levels and molecular structure of LEPs, it is possible to generate a broad spectrum of hues from blue to red by adjusting the absorption and emission spectra [113,114].

Knowing the absorption and emission spectra of LEPs is crucial for the design and optimization of devices that utilize these materials, such as organic light-emitting diodes (OLEDs) and displays. By manipulating the spectral properties

of LEPS, it is feasible to build high-quality, energy-efficient light sources that are suitable for a number of applications and a light-emitting polymer [115,116].

2-10 Laser Induced Fluorescence (LIF) .

Laser-Induced Fluorescence (LIF) involves a two-step process: absorption of a laser photon and subsequent emission of a fluorescence photon from an excited state. The laser wavelength (λ_{Laser}) must align with the permitted energy transition of a LIF-active molecule. Only a fraction of these excited molecules fluoresce, emitting fluorescence light at a red-shifted wavelength (ϕ_{LIF}) [117]. Post relaxation to the ground state, molecules may produce fluorescence quanta with longer wavelengths and exhibit a characteristic average period spent in the excited state, known as the fluorescence lifetime. High-quality optical filters or spectrographs enhance separation between laser and fluorescence wavelengths, optimizing detection sensitivity. Employing lasers with femto-, pico-, Nano-, or microsecond durations allows the determination of the fluorescence lifespan of a sample. [118].

In cases of "prohibited" electronic transitions, excited-state durations of microseconds or milliseconds are seen. Such extended luminescence durations are particularly valuable for bioanalytical applications. The primary focus of fluorescence spectroscopy is on electronic and vibrational states. Typically, the species (molecule of the material) being investigated has a ground electronic state (a state with low energy) of interest and an excited electronic state with a greater energy. There are several vibrational states inside each of these electrical states. In fluorescence, the species is initially stimulated by absorbing a photon from its ground electronic level to one of the several vibrational states in its excited electronic level [119].

The excited molecule loses vibrational energy via collisions with other molecules until it reaches the lowest vibrational state of the excited electronic level [152]. The molecule then rapidly returns to one of the numerous vibrational levels of the ground electronic state, producing a photon in the process (in the range of 10^{-9} s). Since molecules in the ground state may fall to any of multiple vibrational states, the photons released will have varying energy and consequently frequencies [120].

Laser Induced Fluorescence may alternatively be classified as continuous wave or time-resolved LIF. Continuous wave (CW) LIF employs a continuous laser for excitation when just spectral data is needed. A pulsed laser is used to excite the sample in time-resolved LIF, and the sample's emission (either a single wavelength or the whole spectrum) is monitored as a function of time. This gives important time-resolved data, such as the lifetimes of chemical intermediates and their accompanying time-gated spectrum development [121].

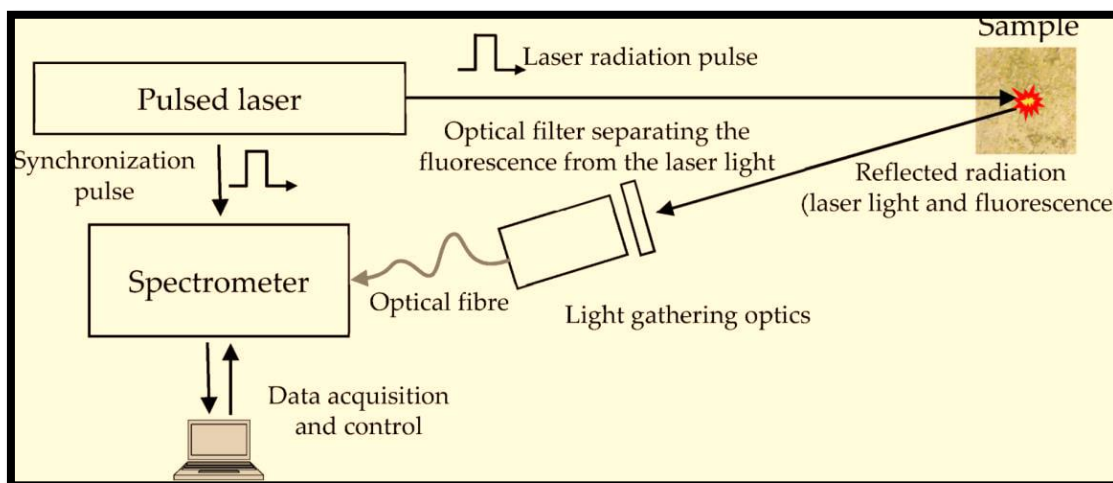


Fig (2-6): Optical devices used in LIF Technology [122].

2-11 Fluorescence Lifetime.

A molecule changes to one of its vibrational levels in the excited electronic state (S_n) when it takes in light from an outside source. The molecule loses part of its vibrational energy and relaxes to a lower vibrational level within the

excited electronic state (S_1) when it collides with nearby molecules in a dense medium (Condensed Phase) [123].

The time taken for the radiative transition from the lowest vibrational level of the excited electronic state (S_1) to one of the vibrational levels in the ground state (S_0), with the system returning to its initial state after this time period, is referred to as the radiative lifetime (τ_{FM}). It is defined as the reciprocal of the radiative transition probability (K_{FM}) in units(sec^{-1}) [124].

$$\tau_{FM} = \frac{1}{K_{FM}} \dots\dots\dots(2-22)$$

(K_{FM}): represents the potential for radioactive transmission.

Due to the presence of non-radiative processes that compete with the radiative transition probability (K_{FM}), fewer molecules will be able to fluoresce. As a result, the total transition probability (K_F) will represent the sum of probabilities for both radiative and non-radiative transitions [125,126].

$$\tau_F = \frac{1}{K_{FM} + \sum K_d} = \frac{1}{K_F} \dots\dots\dots(2-23)$$

($\sum K_d$) is the sum of the non-radiative time rate constants of the lowest vibrational energy level of the excited electronic state (S_1). On the other hand, the fluorescence lifetime (τ_F) is the actual time it takes for fluorescence to occur and is equal to the inverse of the sum of the rate constants of all non-radiative and radiative processes that cause energy losses from the (S_1) state [127,128].

$$\tau_F = \frac{1}{K_{FM} + K_{IC} + K_{ISC}} \dots\dots\dots(2-24)$$

The fluorescence lifetime (τ_F) can serve as the principal lifetime of the excited state. There exists a relationship that links the intensity of fluorescence with the fluorescence lifetime (τ_F). This relationship governs how fluorescence intensity is influenced by the duration of fluorescence emission [129].

$$I = I_0 \exp(-t / \tau_F) \dots \dots \dots (2 - 25)$$

In fluorescence, the intensity (I) represents the fluorescence intensity at a given time (t), while (I₀) represents the highest fluorescence intensity observed, and (t) is the time immediately after excitation ceases. Furthermore, the fluorescence lifetime (F) can be determined from a standard compound with a known fluorescence lifetime value [130].

The (Φ_F -Quantum Yield) represents the quantum yield of fluorescence, which is the ratio between the probability of radiative transition (K_{FM}) and the total energy loss processes of the excited state under specific temperature and environmental conditions [132]. This value is a physical constant specific to each type of excited molecule, or it is the ratio of the total emitted energy to the absorbed energy [131,132].

$$\phi_F = \frac{K_{FM}}{K_{FM} + K_{IC} + K_{ISC}} = \frac{K_{FM}}{K_{FM} + \sum K_d} \dots \dots \dots (2 - 26)$$

where

($\sum K_d$) represents the total number of non-radiative processes constants.

(K_{IC}) represents the internal transformation rate constant.

(K_{ISC}) is the intersystem crossing constant.

In the complete absence of a quenching agent or chemical reactions, the quantitative product of fluorescence (Φ_F) is equal to

$$\phi_F = K_{FM} \tau_F = \frac{\tau_F}{\tau_{FM}} \dots \dots \dots (2-27)$$

It is also possible to calculate the quantitative product of fluorescence (Φ_F) by finding the ratio between the area of the fluorescence spectrum and the area of the absorption spectrum using the equation (2-28) (2-29) [133].

$$\phi_F = \frac{\int F(\nu') d\nu'}{\int \epsilon(\nu') d\nu'} \dots \dots \dots (2-28)$$

$$\tau_F = \frac{a \times \tau_{fPuer}}{a_{Puer}} \dots \dots \dots (2-29)$$

τ_{fpuerr} : Represents the chronological lifetime of the standard compound, which is the light-emitting polymer.

a_{puer} : It is the area under the fluorescence curve of the light-emitting polymer.

a : It represents the area under the curve for the compound required in this research.

It has been observed that the quantum yield of fluorescence for several compounds depends on the excitation wavelength used [134] as well as on the temperature. The quantum yield of fluorescence increases when non-radiative processes decrease and when the temperature decreases, indicating an inverse relationship between them [135]. The values of fluorescence quantum yield range from 1.0 to 0.1, resulting in much shorter fluorescence lifetime (τ_{FM}) values due to competing non-radiative processes. Please note that F refers to the

fluorescence lifetime, which is influenced by the competing non-radiative processes affecting the fluorescence [136].

The fluorescence efficiency and lifetime in light-emitting polymers, such as MEH-PPV and PFO, are influenced by their structural and electronic properties. Polymers with well-defined and rigid conjugated structures tend to exhibit higher fluorescence efficiency [137]. The fluorescence lifetime, which refers to the average time a fluorophore remains in an excited state before returning to its ground state, is associated with slower non-radiative decay processes in light-emitting polymers [138]. Factors like molecular structure, polymer chain packing, and interactions with the surrounding environment can influence the fluorescence properties of MEH-PPV and PFO [139]. By optimizing these factors, researchers can enhance the fluorescence efficiency and lifetime of these light-emitting polymers for various applications, such as organic light-emitting diodes (OLEDs) and optoelectronic devices [140].

Chapter Three

Experimental Part

3.1 Introduction

This chapter includes a step description of the preparation the samples of the light-emitting polymers (MEH-PPV, PFO) and the materials used. It also explains the experimental set-up that is required for laser ablation in liquid. In addition, the techniques used for the characterization of the samples, such as the UV- Vis technique, the fluorescence technique, the FR-SEM, and the LIF technique are presented.

3.2 Materials used in this work

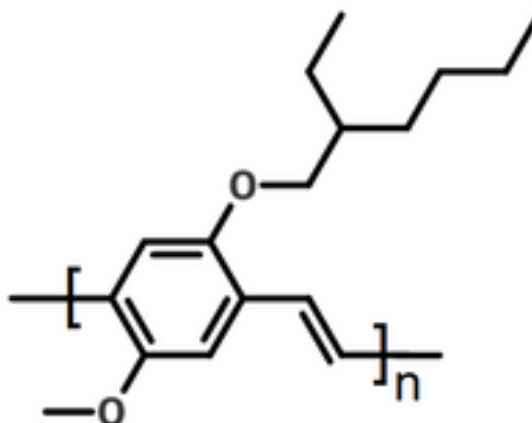
The materials used in this work were purchased from Sigma-Aldrich Company.

3.2.1 The MEH-PPV Polymer

The MEH-PPV is one of the light-emitting polymers, it soluble in organic solvents such as toluene or chlorobenzene, it is considered insoluble in water. The MEH-PPV is powder Orange-Red color. It is one of a PPV derivative that is particularly favorable for electronic devices fabrication because of its asymmetric side chains. The MEH-PPV is possibly one of the most and studied polymer semiconductors, recognizing its many applications, the most important of which is polymer light-emitting diodes (PLED) and perovskite solar cells. Some of the physical and chemical properties of the MEH-PPV are listed in the Table (3-1), the chemical structure is shown in the Fig (3-1).

Table (3-1) the physical and chemical properties of the MEH-PPV [141]

Full name	Poly[2-methoxy-5-(2'-ethylhexyloxy)-1,4-phenylene vinylene]
CAS number	138184-36-8
Chemical formula	$(C_{18}H_{28}O_2)_n$
Solvent	Toluene or chlorobenzene
Melting point	300°C
Appearance	Red fibers/powder
Color	Orange-Red

**Fig (3-1) the chemical structure of the MEH-PPV [142]**

3.2.2 The PFO Polymer

The Polydioctylfluorene (PFO) is one of the light-emitting polymers, it sometimes referred to as poly (9,9-di-n-octylfluorenyl-2,7-diyl), It is an organic compound, a polymer of 9,9-dioctylfluorene, with formula $(C_{13}H_6(C_8H_{17})_2)_n$. The PFO is powder yellow color, it is soluble in organic solvents such as toluene and chloroform, it is an electroluminescent conductive polymer that

characteristically emits blue light, and it has been studied as a possible material for light - emitting diodes.

The PFO is a kind of conjugated polymer, these polymers are distinguished by single and double bonds that alternate, allowing charge to travel throughout the polymer chain. As a result, optoelectronic applications like organic light-emitting diodes (OLEDs) or solar cells might benefit greatly from them [143].

Some of physical and chemical properties of the PFO are listed in the Table (3-2), the chemical structure in the Fig (3-2).

Table (3-2) the physical and chemical properties of the PFO [144].

<i>Full name</i>	<i>(9,9-di-n-octylfluorenyl-2,7-diyl)</i>
<i>CAS number</i>	<i>123864-00-6</i>
<i>Chemical formula</i>	<i>(C₁₃H₆(C₈H₁₇)₂)_n</i>
<i>Solvent</i>	<i>toluene , chloroform</i>
<i>Melting point</i>	<i>60-70 °C</i>
<i>Appearance</i>	<i>Powder</i>
<i>Color</i>	<i>Yellow</i>

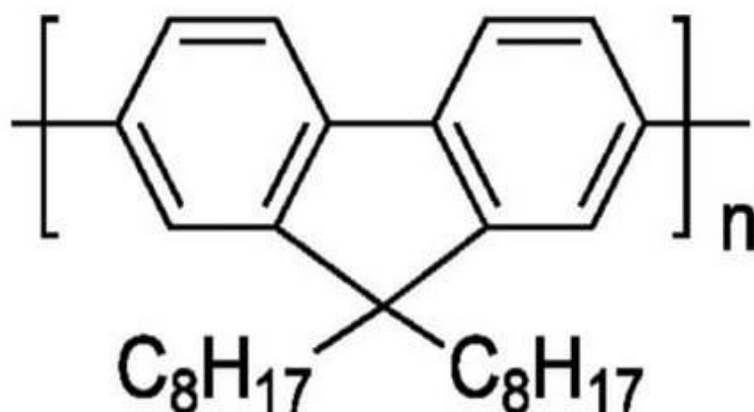


Fig (3-2) the chemical structure of the PFO[145].

3.2.3 The Toluene

Toluene is a substituted aromatic hydrocarbon, it is a colorless, water-insoluble liquid with the odor associated with paint thinners extremely flammable liquid with a pungent, benzene-like odor. It is a mono-substituted benzene derivative, It is belongs to the aromatic hydrocarbon category, consisting of a methyl group (CH₃) attached to a phenyl group. The toluene is a common organic solvent that is sometimes referred to as methylbenzene or phenylmethane. The toluene is predominantly used as an industrial feedstock and a solvent in some types of paint thinner, permanent markers, contact cement and certain types of glue [146].

In our research, the toluene is used as a solvent for the light-emitting polymers such as the MEH-PPV and the PFO. Some of physical and chemical properties of the toluene are listed in the Table (3-3), the chemical structure is presented in the Fig (3-3).

Table (3-3) the physical and chemical properties of the toluene [147].

<i>Full name</i>	<i>Methylbenzene</i>
<i>CAS number</i>	<i>725245</i>
<i>Chemical formula</i>	<i>C₇H₈CH₃</i>
<i>Freezing point</i>	<i>-95°C</i>
<i>Refractive index</i>	<i>1.496</i>
<i>Molecular weight</i>	<i>92.14 gm/mol</i>
<i>Dielectric constant</i>	<i>2.38</i>
<i>Density</i>	<i>0.886 gm/cm³</i>

Toluene | C₇H₈

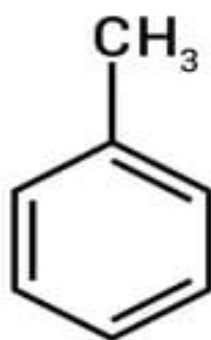


Fig (3-3) the chemical structure of the toluene [148].

3.3: Experimental Part

The experimental work comprises three parts. The first part involves dissolving light-emitting polymers in a solvent at different concentrations. In the second part, the pulsed laser ablation technique is employed to generate Au and Ag in liquid. These metal nanoparticles will subsequently be combined with the light-emitting polymers to investigate the properties of the mixture.

The third part encompasses the utilization of characterization techniques to analyze the samples. The diagram below, Fig (3-4), illustrates the procedural map of the experimental phase in this study.

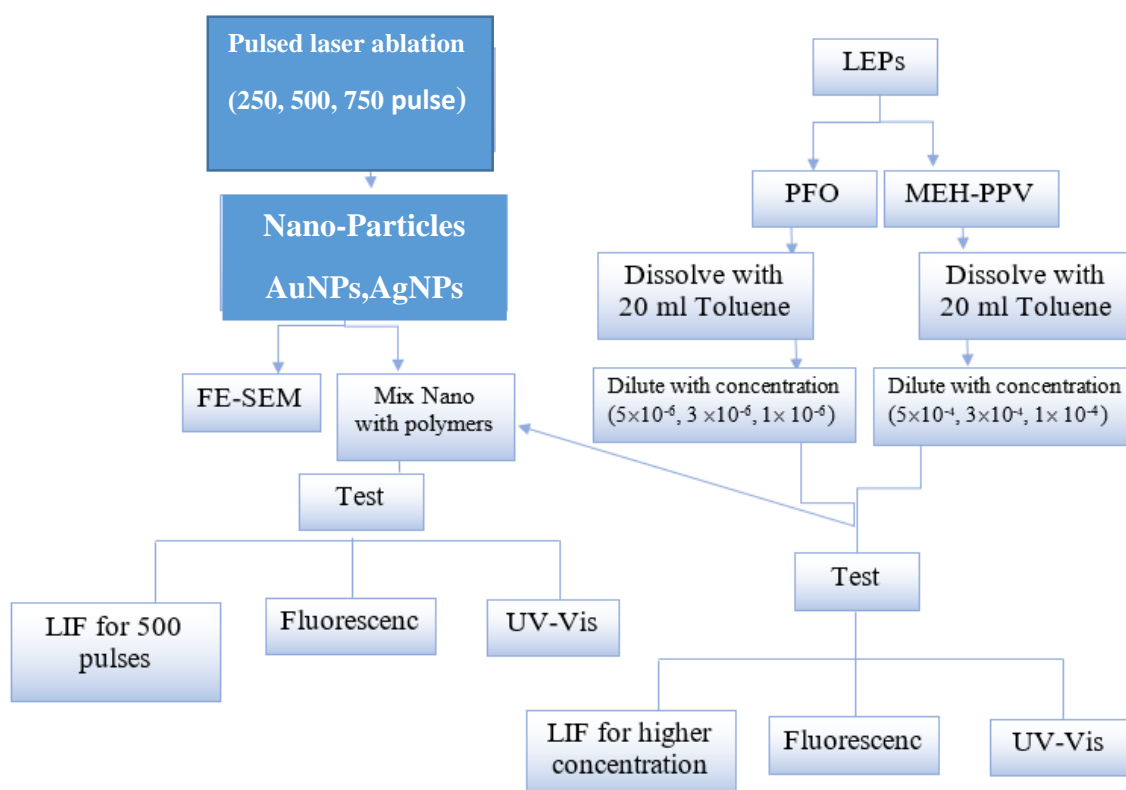


Fig (3-4) the Scheme of the experimental work and the tests those are necessary to describe this work.

3.3.1 Fabrication Technique of Samples: Laser Ablation in Liquids

The experiments were conducted by using the 1064 nm Nd:YAG laser, have 5 ns pulse width, and 6 Hz repetition rate. Energy per pulse was 100 mJ focused directly on the sample placed in a liquid medium. The Fig (3-5) shows the schematic diagram of the experimental setup of laser ablation in liquid media



Fig (3-5) shows a scheme of the experimental setup used in NPs preparation by laser ablation confined in a liquid medium.

The laser pulses were directed at the pure (99.9%) (Au and Ag) (Sigma Aldrich, Germany) metal targets with a thickness of 2 mm, immersed in toluene inside a glass container with a high reflectivity mirror and a lens with focal length 150mm. The height of the toluene over the target was maintained at 10mm. In the meantime, the entire system slowly rotated about its vertical axis during the ablation process to prevent developing of deep holes in the target, and therefore keep the same surface conditions for each laser pulse. Subsequently, the distance between the target and the lens has been set to get the focus point on the target.

3.4 Samples Preparation

Three different concentrations were prepared after dissolving each of the light-emitting polymers (MEH-PPV and PFO) in toluene.

3.4.1 Preparation of the MEH-PPV Samples

1 mg of MEH-PPV polymer is dissolved in 20 ml of the toluene. After that, it is diluted using the weight (3-1) and dilution (3-2) equations to obtain the concentrations ($1 \times 10^{-4} \text{M}$, $3 \times 10^{-4} \text{M}$, and $5 \times 10^{-4} \text{M}$), as in the Fig (3-6). After preparing the polymer concentrations, they are kept in in a dark place to avoid the optical decay.

$$W_m = \frac{C \times V \times Mw}{1000} \quad (3-1)$$

$$C_1 V_1 = C_2 V_2 \quad (3-2)$$

Where:

W_m : the weight of the polymer required to obtain the required concentration in gm.

C : Concentration to be prepared in M; (C_1 : high concentration), (C_2 : Low concentration).

V : volume of solvent in cm^3 added to the substance.

M_w : molecular weight of the polymer used in gm/mol.

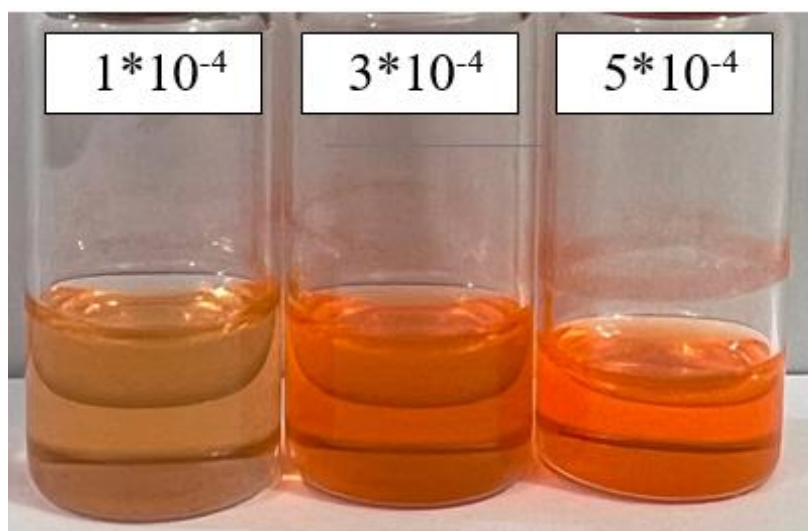


Fig (3-6) the different concentrations of the MEH-PPV polymer.

3.4.2 Samples Preparation of the PFO

The PFO polymer with weight 1 mg is dissolved in 20 ml of the toluene. After that, it is diluted using the weight (3-1) and dilution (3-2) equations to obtain the concentrations (1×10^{-6} M, 3×10^{-6} M, and 5×10^{-6} M), as in the Fig (3-7). After preparing the polymer concentrations, they are kept in a dark place to avoid the optical decay.

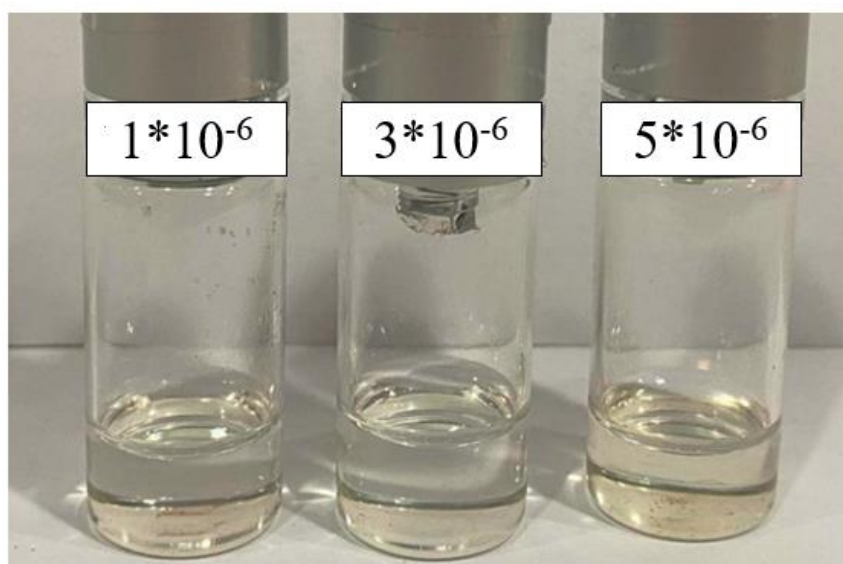


Fig (3-7) the different concentrations of the PFO polymer.

3.4.3 Metallic Nanoparticles Preparation

Two groups of metallic nanoparticles were generated, the first group is the generation of gold nanoparticles (Au NPs) using the pulsed laser ablation technique at three different concentrations, this is done by changing the number of laser pulses (250, 500, and 750 pulse) focused on the gold target.

Likewise, the second group is to generate silver nanoparticles (Ag NPs) at the same three concentrations.

3.4.4 Mixing of metallic nanoparticles with the LEPs

The metallic nanoparticles were mixed with light-emitting polymers in a matrix in a ratio of (1:1), so the highest concentration (750 pulse) of the metallic nanoparticles was chosen to ensure better results. Thus it has three samples of the Au NPs mixed with three concentrations of the MEH-PPV, as in the Fig (3-8a). Similarly, we have three samples of the Ag NPs mixed with three concentrations of the PFO, as in the Fig (3-8b).

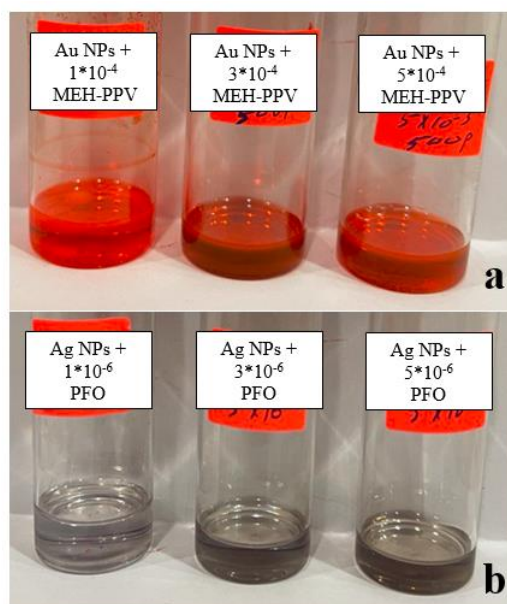


Fig (3-8) the different concentrations of the matrix; a) the Au NPs with the MEH-PPV, and b) the Ag NPs with the PFO.

3.5 Characterization Techniques of Samples:

3.5.1 The Measurement of Absorption Spectra

The linear optical properties of samples have been dedicated by optically transmission and absorption spectra from deep UV to visible region (the wavelength range 190 – 900 nm). The absorption spectra were measured at room temperature using (CE 7400- UV/VIS) double beam spectrophotometer supplied by Aquarius (South Korea) as in Fig (3-9).



Fig (3-9) the UV-Visible Spectrophotometer.

3.5.2 Field Emission Scanning Electron Microscopy (FE-SEM)

In order to investigate the samples NPs shape, size and the thickness, Field Emission Scanning Electron Microscopy was used (FE-SEM) (Σ IGMA, JSM-7610F, Carl Zeiss, Germany) image operating at an accelerating voltage of 10 kV. As shown in Fig (3-10). While the average size of the samples NPs was calculated from FE-SEM images by using Image J software.

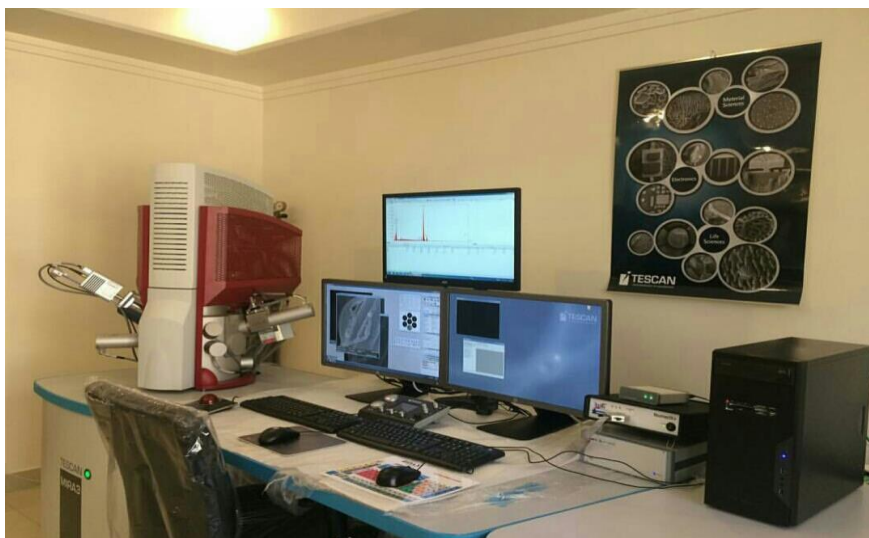


Fig (3-10) Image of the FE-SEM device.

3.5.3 The Measurement of Fluorescence Spectra

The Fluorescence spectrum of the samples were measured by a fluorescence spectrophotometer (model Scinco, FS-2), as presented in Fig (3-11). The Fluorescence spectrometer is comprises of a 150-watt xenon arc lamp with a scan rate of 200, 400, and 600 nm/min. It has emission rate and excitation spectra of 200-700 nm. Also it has a photomultiplier tube (PMT) detector with exceptional sensitivity.



Fig (3-11) Fluorescence Spectrophotometer.

3.5.4 The Measurement of Laser-Induced Fluorescence Spectra

The Laser-Induced Fluorescence Spectra were obtained by exciting fluorescent molecules through the application of the Laser-Induced Fluorescence (LIF) technique. This involved utilizing a continuous-wave laser source with a wavelength of 405 nm. It operates with a power of 30 mill watts. For comparison, there is a continuous-wave laser with a wavelength of 532 nm and a power of 30 mill watts. The LIF provides more accurate measurement of the plasmon-exciton coupling process than a normal fluorescence spectrometer, which uses a regular lamp, because the sample is irradiated with a specific wavelength and the laser irradiance is higher than the regular lamp. The LIF setup contains a laser source, an aperture to regulate the diameter of the laser beam, and an optical lens with a focal length of 10 cm, which is used to focus light on the fiber. The setup is shown in Fig (3-12).

The methodology for laser-induced fluorescence involves placing the specimen on a level surface. Subsequently, light is directed onto the specimen. Following this, a specialized detector captures the fluorescence light, and a computer program is employed to analyze the obtained results.

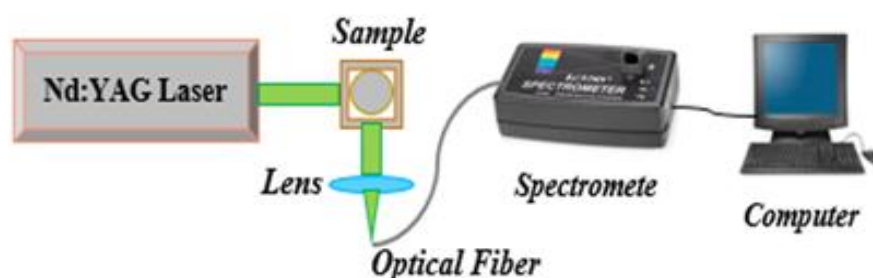


Fig (3-12) the LIF spectroscopy technique.

Chapter Four

Results and Discussion

4.1. Introduction

This chapter includes the results of the experimental measurements of the two kinds of the light-emitting polymers; the MEH-PPV and PFO dissolved in toluene and the discussion of the results.

4.2. Experimental Results

4.2.1. Results of FE-SEM Images

The morphology, size, and shape of the samples were determined by using the FE-SEM images. The Image J software was employed to determine the average sizes of both the Au NPs and the Ag NPs. The average size of the Au NPs and the Ag NPs are ranging from 18 to 35 NPs, The results of the sample morphology exhibit a distinct spherical shapes, as shown in the Fig (4-1).

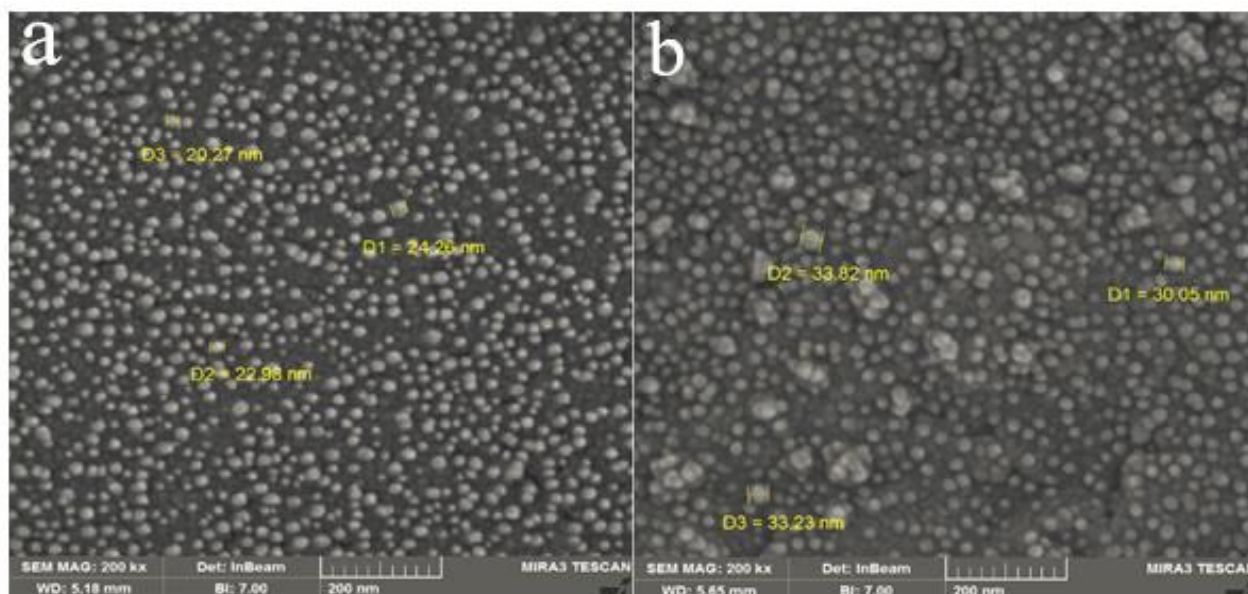


Fig (4-1) the FE-SEM image of; a) the Au NPs, and b) the Ag NPs in the toluene solution.

4.2.2 Results of the optical spectra of the pure MEH-PPV polymer and the pure PFO polymer

The results of the optical spectra measurements of the pure LEPs (MEH-PPV and PFO) dissolved in toluene are shown in the Fig (4-2).

From the results of the absorption spectra of the MEH-PPV polymer we noted the absorption spectra increase when the polymer concentration in toluene increasing, the behavior is depicted in the Fig (4-2a).

Similarly, the absorption spectra of the PFO polymer increases with increasing concentration of the PFO polymer in toluene, as shown in the Fig (4-2b). This is consistent with the Beer-Lambert law, which states that the absorption of a solution is directly proportional to its concentration (assuming the light path length remains constant).

In addition, there is a slight change in the wavelength of absorption peaks with the difference concentration, this the small change in may be due to concentration-dependent phenomena, such as the aggregation of polymer chains, also it can slightly alter the energy levels in the system, and thus affect the light absorption properties.

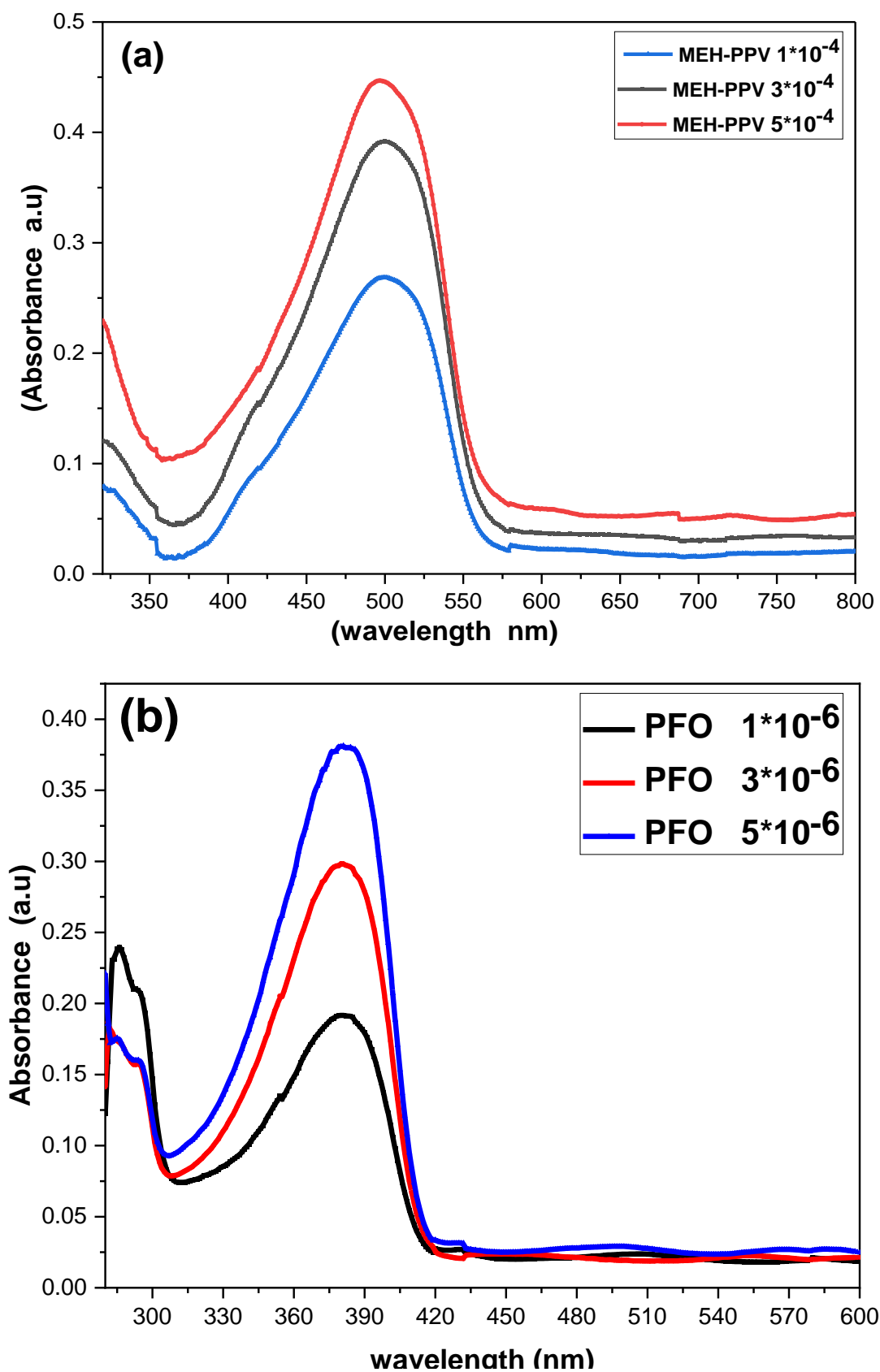


Fig (4-2) the Absorption spectra of a) the pure MEH_PPV in different concentrations, and b) the pure PFO in different concentrations.

4.2.3 Results of the optical spectra of the Au NPs and the Ag NPs

The absorbance of the Au NPs and the Ag NPs generated by the PLAL method increases with increasing number of the laser pulses focused on target (250, 500, and 750 pulses), as shown in Figure (4-3a) for Au NPs and Figure (4-3b) for Ag NPs. There is a small redshift in λ_{\max} of both Au NPs and Ag NPs, as shown in Table (4-1). This could be due to the change in the size of the nanoparticle.

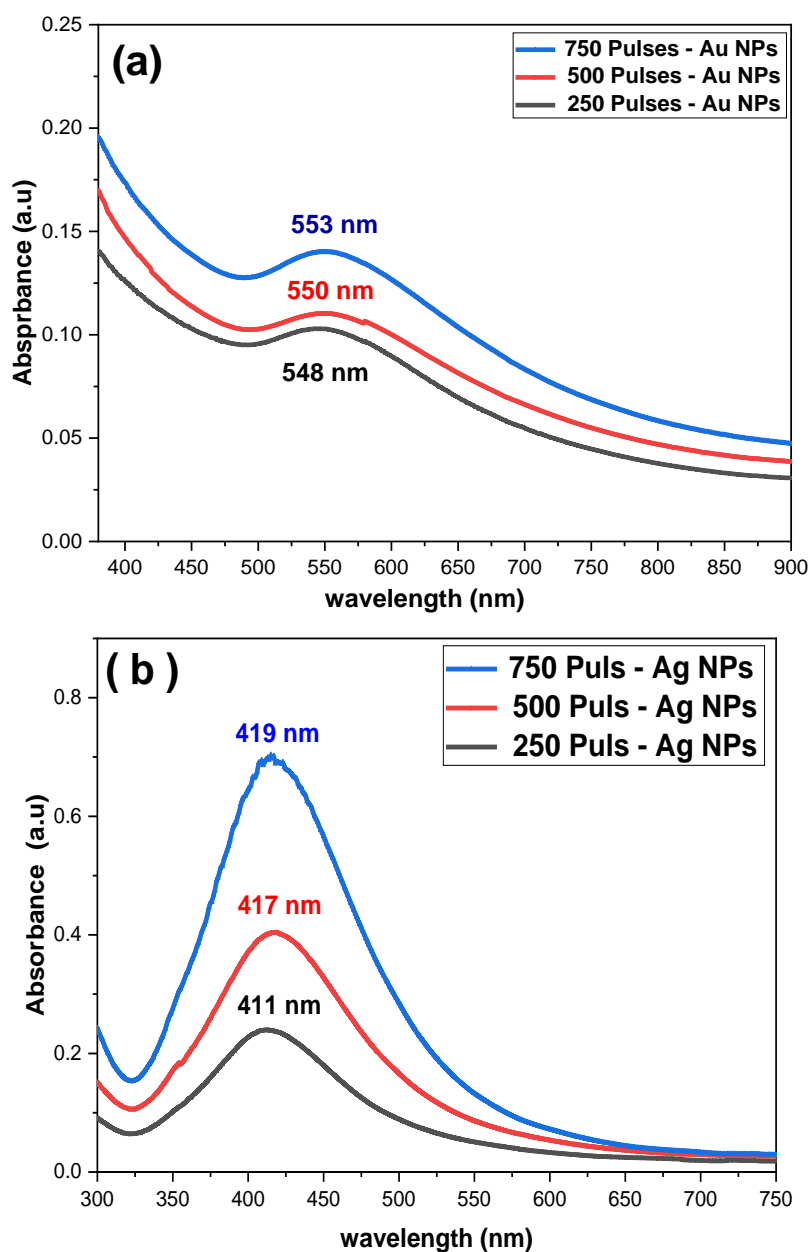


Fig (4-3) the absorption spectra of; a) the Au NPs in different laser pulses, and b) the Ag NPs in different laser pulses.

The results showed that the intensity of absorption increases with increase of concentration of the Au NPs, the behavior is similar for the Ag NPs. This behavior corresponds to a fact that a larger concentration of nanoparticles in the sample leads to providing more sites for photon interactions, thus improving the sample's absorption of light.

Table (4.1) the wavelength shift with changing number of laser pulses.

The number of laser pulses	λ_{\max} (nm)	$\Delta\lambda$ (nm)
250 pulse - Au NPs	548	122
500 pulse - Au NPs	550	119
750 pulse - Au NPs	553	118
250 pulse - Ag NPs	411	165
500 pulse - Ag NPs	417	183
750 pulse - Ag NPs	419	204

4.2.4. Results of the optical spectroscopy of the matrixes (the Au NPs and the Ag NPs with LEPs)

The absorption spectra of the LEP polymers matrix containing metallic nanoparticles are depicted in Figure (4-4).

It can be clearly observed that the intensity of the absorption spectrum of the LEPs are improved, when Au NPs and Ag NPs are added. The highest concentration (750 pulses) of the metallic nanoparticles is selected in order to ensure the size of the generated nanoparticles corresponds to the SPR phenomenon.

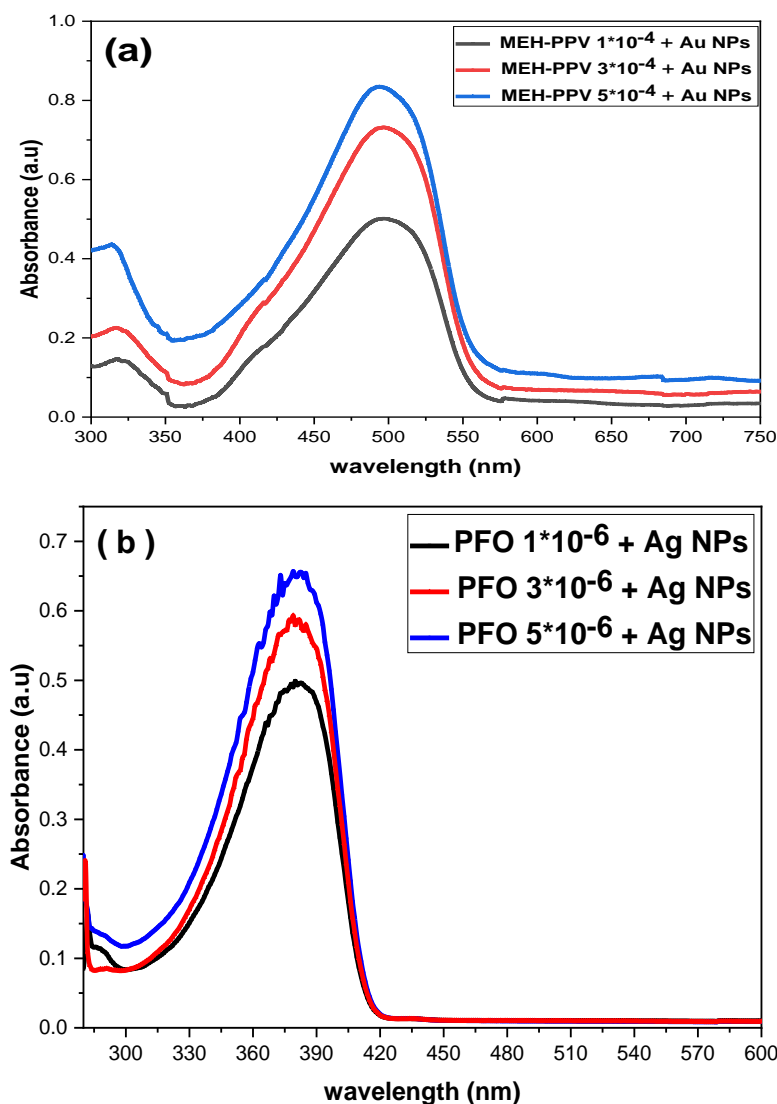


Fig (4-4) the absorption spectrum of; a) the different concentrations of the MEH_PPV with the Au NPs, and b) the different concentrations of the PFO with the Ag NPs.

Notably, the improvement in the optical absorption spectra is due to the addition of the absorbance of the Au NPs and the Ag NPs to the absorption of the polymers.

4.2.5 Results of the fluorescence spectra of the matrix MEH-PPV with Au NPs

The results of the fluorescence spectra of the matrix MEH-PPV with Au NPs are shown in Fig (4-5). The black line displayed on the graph delineates the

baseline fluorescence spectrum of the pure MEH-PPV polymer. The fluorescence spectra exhibit notable changes upon the addition of Gold Nanoparticles (Au NPs) with different concentrations. The impact of introducing Au NPs on enhancing the fluorescence spectra of the MEH-PPV polymer is evident. This improvement becoming more pronounced as the concentration of Au NPs increases. However, at higher concentrations of Au NPs, specifically for 750 pulses, a slight decline in the fluorescence spectrum is observed. This decline is attributed to the phenomenon of quenching, resulting in the suppression of spectra across all concentrations of the polymer employed in the study.

The augmentation of fluorescence implies a synergistic interaction between the metallic nanoparticles and the polymer, possibly facilitated through mechanisms such as surface enhancement effects or energy transfer processes [149].

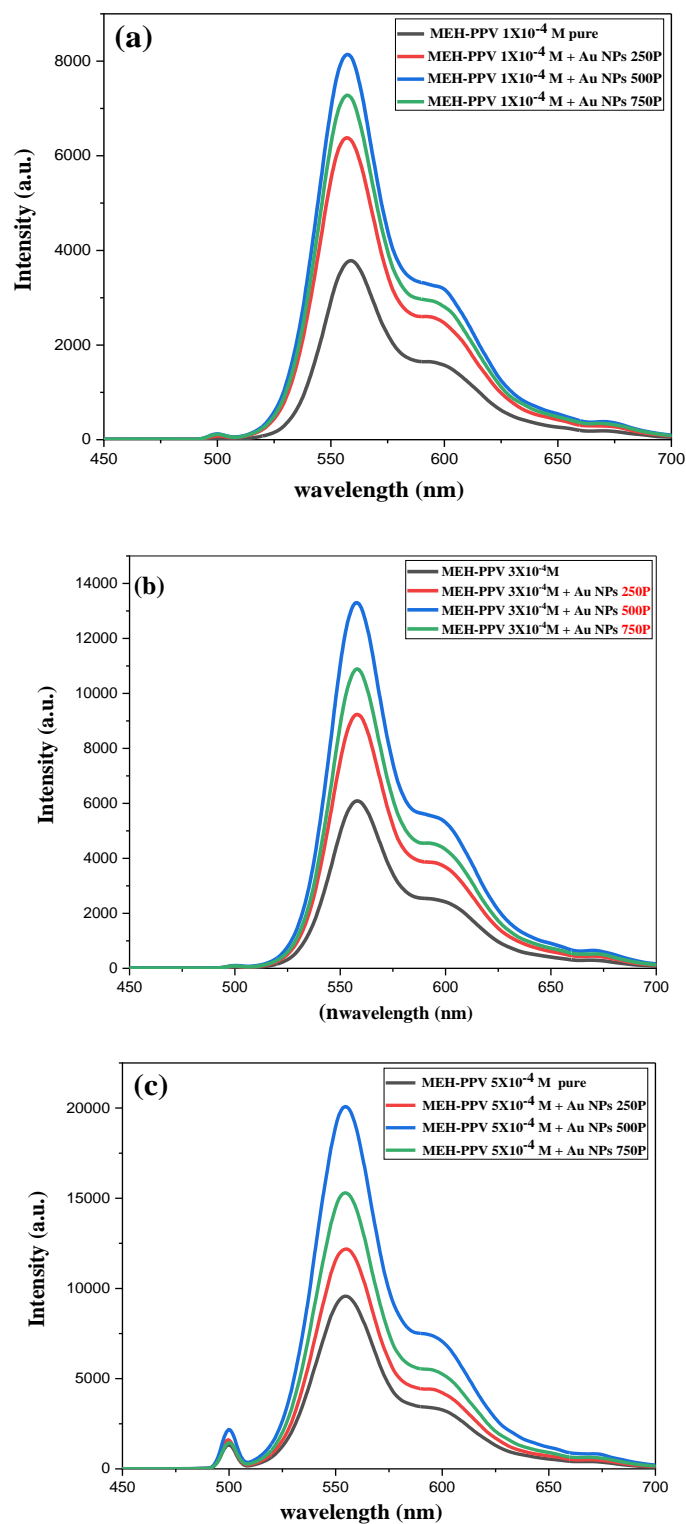


Fig (4-5) the fluorescence spectra of the MHE-PPV polymer with the Au NPs at different concentrations; a) 1×10^{-4} M, b) 3×10^{-4} M, and c) 5×10^{-4} M.

4.2.6 Results of the fluorescence spectra of the matrix PFO with the Ag NPs

The results of the fluorescence spectra of the PFO with Ag NPs are shown in the Fig (4-6). The behavior is as expected, adding the Ag NPs to the PFO polymer matrix leads to an increase in the intensity of fluorescence. This improvement increases when the concentration of the Ag NPs increases. However, for the samples prepared with 750 pulses the fluorescence slightly decreases. This reduction could be due to the phenomenon of quenching. The quenching, in this context, refers to the process by which higher concentrations of nanoparticles can lead to a reduced emission of light, essentially 'quenching' the fluorescence. This could be due to mechanisms such as non-radiative energy transfers or the reabsorption of emitted light by excessive nanoparticles.

In light of these observations, we can conclude that the optimal emission spectrum for the PFO polymer, in terms of maximum fluorescence intensity, is achieved with a nanoparticle concentration of 500 P. This provides a key understanding for tailoring the properties of the PFO polymer with nanoparticle additives for various applications, including optoelectronics and sensing devices.

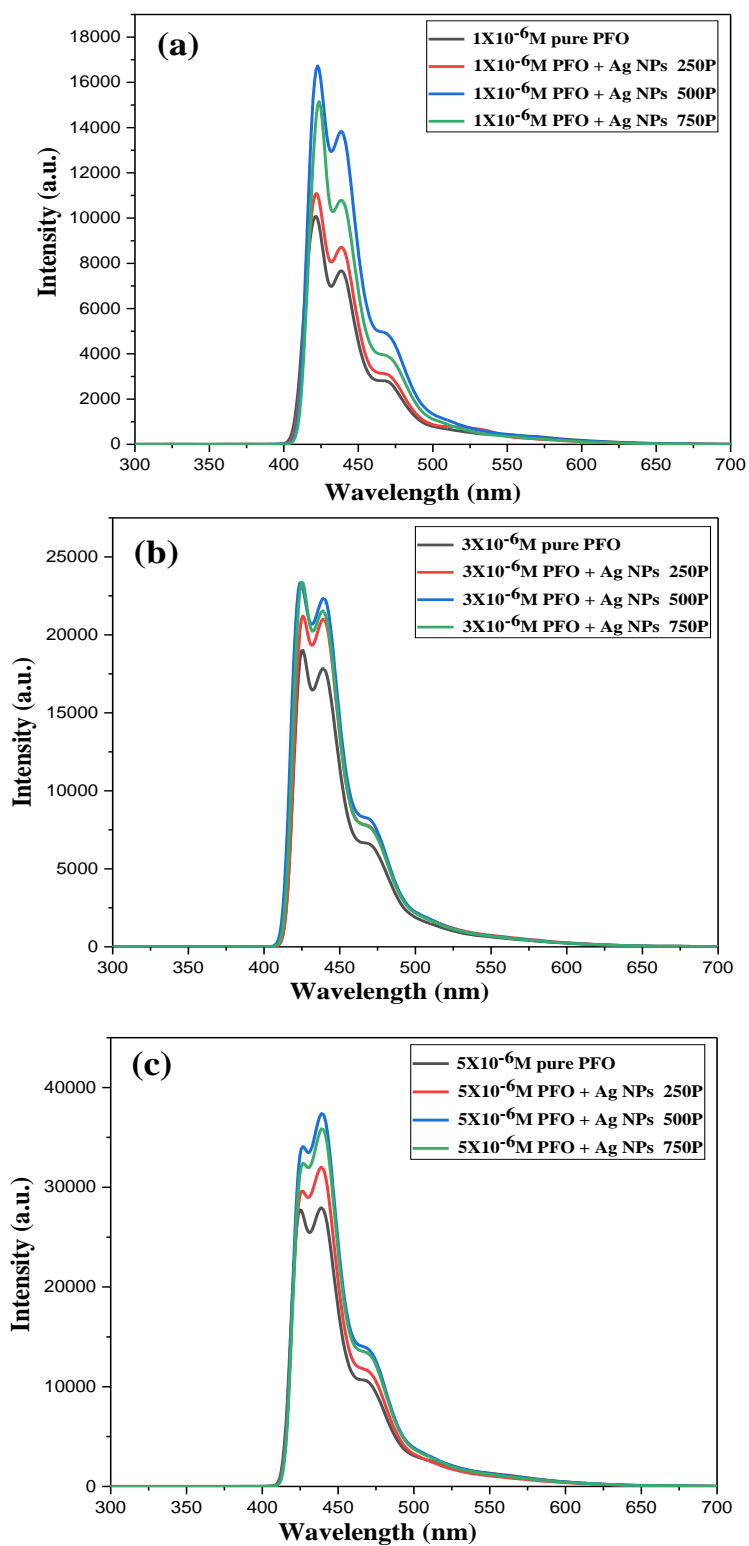


Fig (4-6) the fluorescence spectra of the PFO polymer with the Ag NPs at different concentrations; a) $1 \times 10^{-6} M$, b) $3 \times 10^{-6} M$, and c) $5 \times 10^{-6} M$.

The fluorescence spectra indicate two emission peaks from the pure polymer, likely due to distinct electronic transitions within the polymer molecules [149]. The first peak is thought to represent the initial emission of the polymer, while the second peak could be associated with additional excited states or interactions within the material. When the Ag NPs are introduced into the polymer, an increase in intensity is observed for the two peaks in the fluorescence spectrum. This improvement in the fluorescence can be attributed to the well-known phenomenon of the fluorescence intensification by the metallic nanoparticles, which is typically associated with the plasmon - exciton coupling.

4.2.7 Results of the laser-induced fluorescence of the matrix MEH-PPV with the Au NPs

The results of the LIF spectra of the pure MEH-PPV polymer and the MEH-PPV polymer with Au NPs is shown in the Fig (4-7). The samples were excited at a wavelength of 405 nm to get these spectra, they are also compared to wavelength 532 nm to demonstrate the effect of wavelength on the results.

Based on the results, adding the Au NPs led to a clear improvement in the LIF spectrum under the 405 nm laser illumination, as shown in Fig (4-7a). This behavior may be explained by the fact that the Au NPs function as localized surface plasmon resonators. With the help of plasmon - exciton coupling, they may improve the polymer's emission characteristics. The observed peaks in the LIF spectra may be attributed to energy transfer mechanisms that are induced by the interaction between the MEH-PPV polymer and the Au NPs [149]. The coupling between plasmon-exciton promotes more effective energy transfer mechanisms, as a consequence improves the LIF emission properties. The LIF emissions of the MEH-PPV polymer at wavelength 532 nm shown in the Fig (4-7b). It can be clearly observed that the improvement occurring in the LIF

spectra under the influence of the green wavelength is better compared to the blue wavelength, due to the SPR phenomenon of the Au NPs that directly corresponds to the green wavelength.

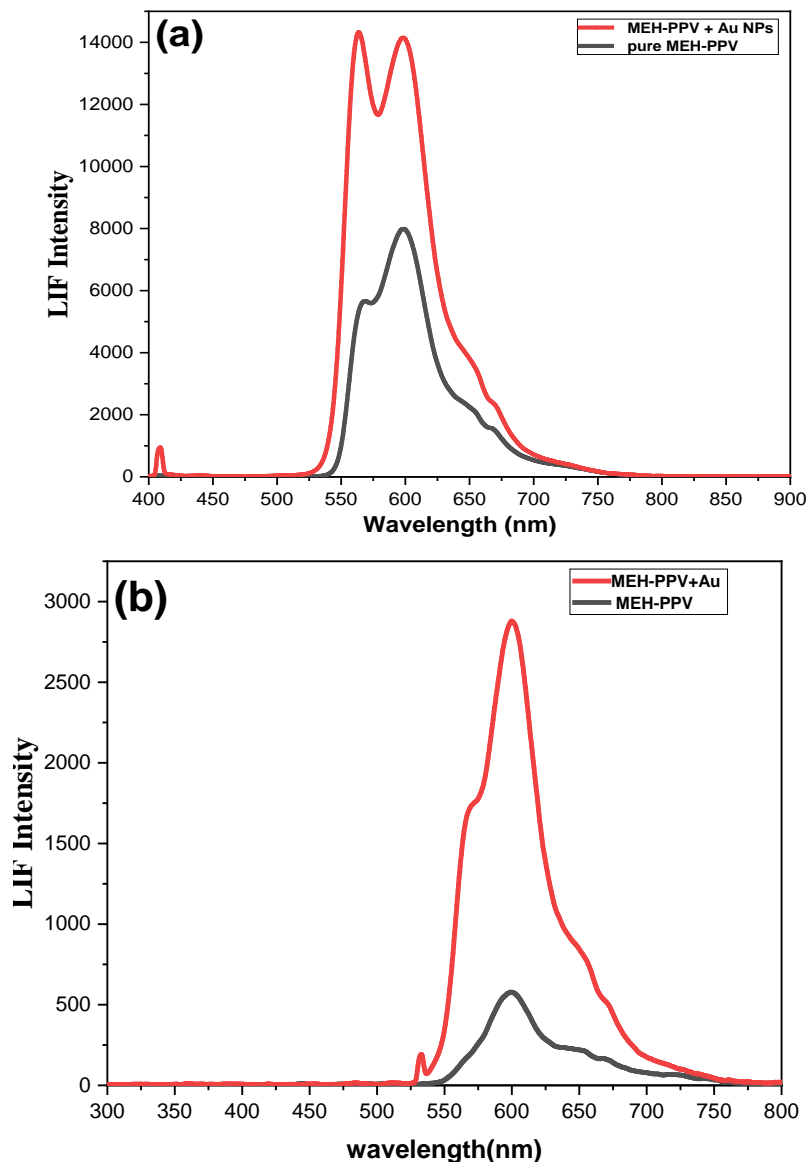


Fig (4-7) the LIF spectra of the pure MEH-PPV polymer compared to the doped MEH-PPV polymer, of the wavelength-excited; a) 405 nm, and b) 532 nm.

Thus, when the polymer is excited at a wavelength of 532 nm, it absorbs more energy due to the presence of the Au NPs. This amplified absorption and more efficient energy transfer led to an increased intensity of the emitted light,

accounting for the observed increase in luminescence intensity. This enhancement contributes could have significant implications for industries reliant on luminescence, including the manufacturing of the Light-Emitting Diodes (LEDs), the development of sensors, and bio-imaging.

4.2.8 Results of the laser-induced fluorescence of the matrix PFO with the Ag NPs

The results of the effect of adding the Ag NPs to the PFO polymer on the LIF spectra are shown in Fig (4-8). The noticeable improvement in the LIF spectra intensity as well as the redshift in wavelength that the Ag NPs cause to the matrix compared to the pure polymer under the influence of the 405 nm wavelength are shown in Fig (4.8). It is actually caused by the interaction between the plasmon and the exciton.

The presence of the Ag NPs can lead to enhance light emission, which indicates more efficient energy transfer between the excitons in the PFO polymer and the plasmons in the Ag NPs. The Ag NPs interact with excitons in the polymer, resulting in intense photoemission, the specific size, shape, and distribution of the Ag NPs within the polymer matrix can influence the strength of this coupling, which in turn affects the fluorescence properties of the PFO polymer. Attributed to changes in the local electromagnetic field caused by plasmonic coupling. These changes may lead to altered exciton energy levels or modified radioactive decay pathways within the polymer, leading to the observed spectral shift. It can be clearly seen that the fluorescence spectra contain two peaks, likely due to distinct electronic transitions within the polymer molecules. The first peak is thought to represent the initial emission of the polymer, while the second peak could be associated with additional excited states or interactions within the material. When the Ag NPs are introduced into the PFO polymer, an increase in intensity is observed for both peaks in the fluorescence spectrum for

all concentrations compared to the pure polymer. This improvement in fluorescence can be attributed to the well-known phenomenon of fluorescence intensification by metallic nanoparticles, which is typically associated with the SPR.

Overall, the results indicate that the incorporation of the Ag NPs into the PFO can enhance the fluorescence intensity and broaden the emission bandwidth, demonstrating the potential of the plasmon-exciton coupling as a means to improve the optical properties of the light-emitting polymers. Further investigations and optimizations of the silver nanoparticle concentration, size, and morphology can be explored to achieve more significant improvements in the fluorescence properties of the polymer.

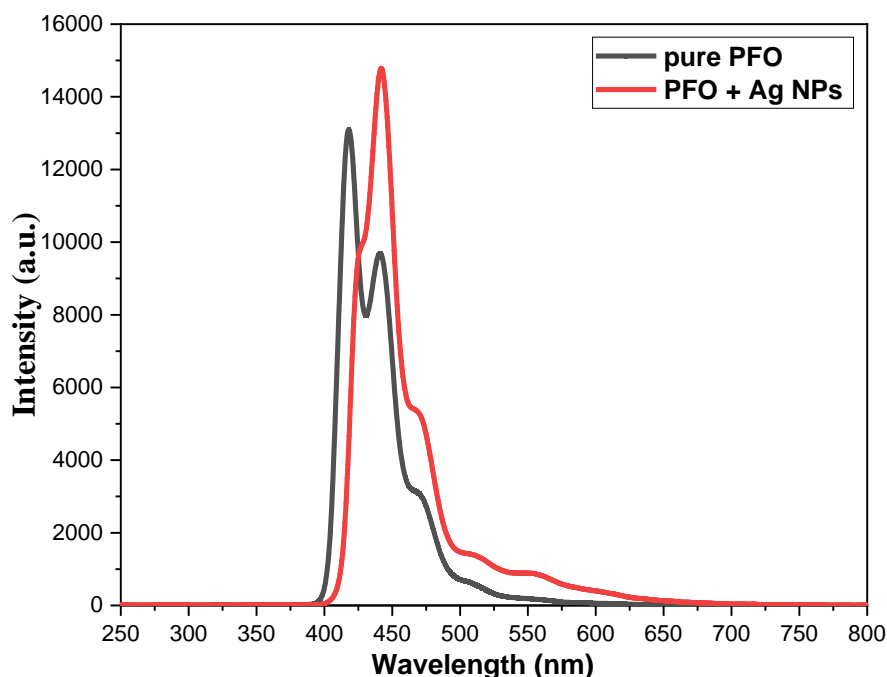


Fig (4-8) the LIF spectra of the pure PFO polymer compared to the doped PFO polymer of the wavelength 405 nm.

4.2.9 Results of the Quantum Efficiency of the LEP MEH-PPV

Through the results of the fluorescence spectra, it was possible to calculate the relative quantum efficiency of the fluorescence (Qf). After calculating the area under the curve for the absorption and fluorescence curves, the results were as shown in Table (4.1), for the MEH-PPV polymer at different concentrations after adding Au NPs. The improvement is calculated relative to the fluorescence quantum yield of the pure.

Table (4-2) the improvement in the quantum efficiency of the MEH-PPV after adding nanoparticles the Au NPs at all concentrations.

<i>Concentrations (M)</i>	<i>The improvement in the quantum efficiency</i>
$1 \cdot 10^{-4}$	31%
$3 \cdot 10^{-4}$	33%
$5 \cdot 10^{-4}$	35%

Similarly, the results of the quantum efficiency of fluorescence of the PFO at different concentrations, after adding Ag NPs, it displayed in it is Table (4-2).

Table (4-3) The improvement in the quantum efficiency of the PFO after adding nanoparticles the Ag NPs at all concentrations.

<i>Concentrations (M)</i>	<i>The improvement in the quantum efficiency</i>
$1 \cdot 10^{-6}$	20%
$3 \cdot 10^{-6}$	28%

5×10^{-6}	31%
--------------------	-----

is clearly observed from the Table (4-2) and the Table (4-3) that the LEP polymers concentration has a direct effect on the quantum efficiency of fluorescence results. Indeed, the metal nanoparticles have a positive effect on the quantum efficiency properties, this effect increases with increasing concentration. The metal nanoparticles play an additional absorption sources based on the SPR phenomenon.

In addition to, the plasmon-exciton coupling between the Au NPs and the MEH-PPV, and between the Ag NPs and the PFO leads to an improvement in the overall optical properties of the LEPs. These improvements include increase in the quantum efficiency for both LEP polymers for all concentrations.

Chapter Five

Conclusion & Future Works

5-1: Conclusion

From this study, we can conclude the following: -

- 1- Our results show significant adjustability of absorption intensity by using nanoparticles. This may be useful in the design of optical absorption devices.
- 2- The Light-emitting polymers mixed with nanoparticles lead to increase fluorescence intensity and slightly change the width of the emission spectrum.
- 3- The LIF spectra reveal a synergistic effect between plasmon excitation and the photopolymer, leading to enhanced light emission efficiency.
- 4- Accordingly, the results show the possibility of using the LEPs enhanced in many applications, especially in the development of optical devices and detectors.

5-2: Future Works.

1-Enhancing the optical and electrical properties of a light-emitting polymers by doping with semiconductor nanomaterials.

2-Studying hybrid structures of a light-emitting polymers and improving their optical and electrical properties.

3-Improving the nonlinear optical properties of a light-emitting polymers used as optical detectors.

4-Using multilayer films of a light-emitting polymers to develop the optical devices.

5-Using of light-emitting polymers doped with plasmonic nanostructures as active media in solid-state lasers.

Reference

Reference

- [1] Muccini, M., & Toffanin, S. (2016). *Organic light-emitting transistors: towards the next generation display technology*. John Wiley & Sons.
- [2] Thejo Kalyani, N., and S.J. Dhoble. "Novel materials for fabrication and encapsulation of OLEDs." *Renewable and Sustainable Energy Reviews* 44 (2015), 319-347.
- [3] Jiang, Tingcong, Yuchao Liu, Zhongjie Ren, and Shouke Yan. "The design, synthesis and performance of thermally activated delayed fluorescence macromolecules." *Polymer Chemistry* 11, no. 9 (2020), 1555-1571.
- [4] Chen, Yujie, Johannes Herrnsdorf, Benoit Guilhabert, Yanfeng Zhang, Alexander L. Kanibolotsky, Peter J. Skabara, Erdan Gu, Nicolas Laurand, and Martin D. Dawson. "Modification of emission wavelength in organic random lasers based on photonic glass." *Organic Electronics* 13, no. 7 (2012), 1129-1135.
- [5] Kik, P. G., & Brongersma, M. L. (2007). Surface plasmon nanophotonics. In *Surface Plasmon Nanophotonics* (pp. 1-9). Dordrecht: Springer Netherlands.
- [6] Tokel, Onur, Fatih Inci, and Utkan Demirci. "Advances in Plasmonic Technologies for Point of Care Applications." *Chemical Reviews* 114, no. 11 (2014), 5728-5752.
- [7] Kravets, V. G., A. V. Kabashin, W. L. Barnes, and A. N. Grigorenko. "Plasmonic Surface Lattice Resonances: A Review of Properties and Applications." *Chemical Reviews* 118, no. 12 (2018), 5912-5951.
- [8] Linic, Suljo, Phillip Christopher, and David B. Ingram. "Plasmonic-metal nanostructures for efficient conversion of solar to chemical energy." *Nature Materials* 10, no. 12 (2011), 911-921.
- [9] Naik, Gururaj V., Vladimir M. Shalaev, and Alexandra Boltasseva. "Alternative Plasmonic Materials: Beyond Gold and Silver." *Advanced Materials* 25, no. 24 (2013), 3264-3294.
- [10] Gonçalves, P. A., and F. J. García de Abajo. "Multi-plasmon effects and plasmon satellites in photoemission from nanostructures." *Nanoscale* 15, no. 28 (2023), 11852-11859.
- [11] Kim, Hyoung-il, Seunghyun Weon, Homan Kang, Anna L. Hagstrom, Oh S. Kwon, Yoon-Sik Lee, Wonyong Choi, and Jae-Hong Kim. "Plasmon-Enhanced Sub-Bandgap Photocatalysis via Triplet–Triplet Annihilation Upconversion for

- Volatile Organic Compound Degradation." *Environmental Science & Technology* 50, no. 20 (2016), 11184-11192.
- [12] Lin, Weihua, En Cao, Liqiang Zhang, Xuefeng Xu, Yuzhi Song, Wenjie Liang, and Mengtao Sun. "Electrically enhanced hot hole driven oxidation catalysis at the interface of a plasmon–exciton hybrid." *Nanoscale* 10, no. 12 (2018), 5482-5488.
- [13] Szychowski, Brian, Matthew Pelton, and Marie-Christine Daniel. "Preparation and properties of plasmonic-excitonic nanoparticle assemblies." *Nanophotonics* 8, no. 4 (2019), 517-547.
- [14] Vaskin, Aleksandr, Radoslaw Kolkowski, A. F. Koenderink, and Isabelle Staude. "Light-emitting metasurfaces." *Nanophotonics* 8, no. 7 (2019), 1151-1198.
- [15] Faleiros, Marcelo M., and Paulo B. Miranda. "Photoluminescence of MEH-PPV with ultraviolet excitation." *Synthetic Metals* 160, no. 23-24 (2010), 2409-2412.
- [16] Zhang, Y., Li, Y., Gao, W., Chen, Y., and Zhang, L. "Silver nanoparticle-enhanced emission of poly(9,9-dioctylfluorenyl-2,7-diyl) for organic light-emitting diodes." *ACS Applied Materials & Interfaces* 5, no. 18 (2013).
- [17] Mucur, Selin P., Tülay A. Tumay, Sait E. San, and Emine Tekin. "Enhancing effects of nanoparticles on polymer-OLED performances." *Journal of Nanoparticle Research* 14, no. 10 (2012).
- [18] Wu, Xiaoyan, Linlin Liu, Zhicong Deng, Li Nian, Wenzhuo Zhang, Dehua Hu, Zengqi Xie, Yueqi Mo, and Yuguang Ma. "Efficiency Improvement in Polymer Light-Emitting Diodes by “Far-Field” Effect of Gold Nanoparticles." *Particle & Particle Systems Characterization* 32, no. 6 (2015), 686-692.
- [19] Aziz, T.H.T., M.M. Salleh, N.A. Bakar, A.A. Umar, and M.Y.A. Rahman. "Electroluminescence Enhancement of Polymer Light Emitting Diodes Through Surface Plasmons by Ag Nanoplates." *Acta Physica Polonica A* 129, no. 4 (2016),
- [20] Stolz, Sebastian, Yingjie Zhang, Uli Lemmer, Gerardo Hernandez-Sosa, and Hany Aziz. "Degradation Mechanisms in Organic Light-Emitting Diodes with Polyethylenimine as a Solution-Processed Electron Injection Layer." *ACS Applied Materials & Interfaces* 9, no. 3 (2017), 2776-2785.

- [21] Wang, Ruizhi, Xiao Yang, Shu Hu, Yang Zhang, Xiaoliang Yan, Yuchen Wang, Chuang Zhang, and ChuanXiang Sheng. "Effect of Thermal Annealing on Aggregations in MEH-PPV Films." *The Journal of Physical Chemistry C* 123, no. 17 (2019), 11055-11062.
- [22] Tooba, Siddiqui., Mohammad, Khalid, Zia., Mohammad, Muaz., Haseeb, Ahsan., Fahim, Halim, Khan. (2022). Interaction of Silver Nanoparticles with Human Alpha-2-macroglobulin: Biochemical and Biophysical Investigation. *MCBS (Molecular and Cellular Biomedical Sciences)*
- [23] Disorder in P3HT Nanoparticles Probed by Optical Spectroscopy on P3HTbPEG Micelles." (n.d.) (2019).
- [24] Kesavan, A. V., Rao, A. D., & Ramamurthy, P. C. (2020). Tailoring optoelectronic properties of CH₃NH₃PbI₃ perovskite photovoltaics using al nanoparticle modified PC61BM layer. *Solar Energy*, 201, 621-627.
- [25] Suheil, S. A., N. S. Shnan, and Qussay Mohammed Salman. "The Plasmon Effects of AgNPs on Wave Guide Consisting of Polymers Mixed with Rhodamine Dyes." *Journal of Physics: Conference Series* 1829, no. 1 (2021), 012007.
- [26] Mohammed, S.H., and N.S. Shanan. "Imaging of Surface Plasmon Resonance for Nano Material of Different Shapes." *Journal of Physics: Conference Series* 1999, no. 1 (2021), 012149.
- [27] Haddawi, S.F., A.K. Kodeary, N.S. Shnan, Hammad R. Humud, and S.M. Hamidi. "Light emitting polymers in two dimensional plasmonic multi wavelength random laser." *Optik* 231 (2021), 166437.
- [28] Suheil, S. A., N. S. Shnan, and Qussay Mohammed Salman. "The Plasmon Effects of AgNPs on Wave Guide Consisting of Polymers Mixed with Rhodamine Dyes." *Journal of Physics: Conference Series* 1829, no. 1 (2021), 012007.
- [29] Zhao, Y., Zhang, J., Li, B., Cheng, X., and Chen, Y. "Plasmon-enhanced photoluminescence of organic polymers with different doping concentrations." *Journal of Materials Chemistry C* 9, no. 5 (2021): 2263-2271.
- [30] Mishra, Gyan P., Dharmendra Kumar, Vijay S. Chaudhary, and Santosh Kumar. "Design and Sensitivity Improvement of Microstructured-Core Photonic Crystal Fiber Based Sensor for Methane and Hydrogen Fluoride Detection." *IEEE Sensors Journal* 22, no. 2 (2022), 1265-1272.

- [31] Amendola, Vincenzo, Roberto Pilot, Marco Frasconi, Onofrio M. Maragò, and Maria A. Iatì. "Surface plasmon resonance in gold nanoparticles: a review." *Journal of Physics: Condensed Matter* 29, no. 20 (2017), 203002.
- [32] Altug, Hatice, Sang-Hyun Oh, Stefan A. Maier, and Jiří Homola. "Advances and applications of nanophotonic biosensors." *Nature Nanotechnology* 17, no. 1 (2022), 5-16.
- [33] Nurrohman, Devi T., and Nan-Fu Chiu. "A Review of Graphene-Based Surface Plasmon Resonance and Surface-Enhanced Raman Scattering Biosensors: Current Status and Future Prospects." *Nanomaterials* 11, no. 1 (2021), 216.
- [34] Lee, ByoungHo, Il-Min Lee, Seyoon Kim, Dong-Ho Oh, and Lambertus Hesselink. "Review on subwavelength confinement of light with plasmonics." *Journal of Modern Optics* 57, no. 16 (2010), 1479-1497.
- [35] Li, Ming, Scott K. Cushing, and Nianqiang Wu. "Plasmon-enhanced optical sensors: a review." *The Analyst* 140, no. 2 (2015), 386-406.
- [36] Liang, Zhiqiang, Jun Sun, Yueyue Jiang, Lin Jiang, and Xiaodong Chen. "Plasmonic Enhanced Optoelectronic Devices." *Plasmonics* 9, no. 4 (2014), 859-866.
- [37] Zhang, Junxi, Lide Zhang, and Wei Xu. "Surface plasmon polaritons: physics and applications." *Journal of Physics D: Applied Physics* 45, no. 11 (2012), 113001.
- [38] Das, Gobind, Salma Alrasheed, Maria L. Coluccio, Francesco Gentile, Annalisa Nicastrì, Patrizio Candeloro, Giovanni Cuda, Gerardo Perozziello, and Enzo Di Fabrizio. "Few molecule SERS detection using nanolens based plasmonic nanostructure: application to point mutation detection." *RSC Advances* 6, no. 109 (2016), 107916-107923.
- [39] Amendola, Vincenzo, Roberto Pilot, Marco Frasconi, Onofrio M. Maragò, and Maria A. Iatì. "Surface plasmon resonance in gold nanoparticles: a review." *Journal of Physics: Condensed Matter* 29, no. 20 (2017), 203002.
- [40] Sun, Lu, Ping Chen, and Lie Lin. "Enhanced Molecular Spectroscopy via Localized Surface Plasmon Resonance." *Applications of Molecular Spectroscopy to Current Research in the Chemical and Biological Sciences*, 2016.
- [41] Dobson, Peter J. "Introduction to Metal-nanoparticle Plasmonics, by Matthew Pelton and Garnett W. Bryant." *Contemporary Physics* 55, no. 4 (2014), 352-353.

- [42] Kampfrath, Tobias, Koichiro Tanaka, and Keith A. Nelson. "Resonant and nonresonant control over matter and light by intense terahertz transients." *Nature Photonics* 7, no. 9 (2013), 680-690.
- [43] Maier, Stefan A. "Plasmon Waveguides." *Plasmonics: Fundamentals and Applications*, 2007, 109-139.
- [44] Amendola, Vincenzo, Roberto Pilot, Marco Frasconi, Onofrio M. Maragò, and Maria A. Iatì. "Surface plasmon resonance in gold nanoparticles: a review." *Journal of Physics: Condensed Matter* 29, no. 20 (2017), 203002.
- [45] Homola, Jiri. "ChemInform Abstract: Surface Plasmon Resonance Sensors for Detection of Chemical and Biological Species." *ChemInform* 39, no. 18 (2008).
- [46] Ni, Weihai, Xiaoshan Kou, Zhi Yang, and Jianfang Wang. "Tailoring Longitudinal Surface Plasmon Wavelengths, Scattering and Absorption Cross Sections of Gold Nanorods." *ACS Nano* 2, no. 4 (2008), 677-686.
- [47] Linardy, Eric, Dinesh Yadav, Daniele Vella, Ivan A. Verzhbitskiy, Kenji Watanabe, Takashi Taniguchi, Fabian Pauly, Maxim Trushin, and Goki Eda. "Harnessing Exciton–Exciton Annihilation in Two-Dimensional Semiconductors." *Nano Letters* 20, no. 3 (2020), 1647-1653.
- [48] Salén, Peter, Martina Basini, Stefano Bonetti, János Hebling, Mikhail Krasilnikov, Alexey Y. Nikitin, Georgii Shamuilov, Zoltán Tibai, Vitali Zhaunerchyk, and Vitaliy Goryashko. "Matter manipulation with extreme terahertz light: Progress in the enabling THz technology." *Physics Reports* 836-837 (2019), 1-74.
- [49] Wang, Danqing, Jun Guan, Jingtian Hu, Marc R. Bourgeois, and Teri W. Odom. "Manipulating Light–Matter Interactions in Plasmonic Nanoparticle Lattices." *Accounts of Chemical Research* 52, no. 11 (2019), 2997-3007.
- [50] Lee, Jihye, Deok-Jin Jeon, and Jong-Souk Yeo. "Quantum Plasmonics: Energy Transport Through Plasmonic Gap." *Advanced Materials* 33, no. 47 (2021).
- [51] He, Zhicong, Fang Li, Yahui Liu, Fuqiang Yao, Litu Xu, Xiaobo Han, and Kai Wang. "Principle and Applications of the Coupling of Surface Plasmons and Excitons." *Applied Sciences* 10, no. 5 (2020), 1774.
- [52] Munkhbat, Battulga, Martin Wersäll, Denis G. Baranov, Tomasz J. Antosiewicz, and Timur Shegai. "Suppression of photo-oxidation of organic chromophores by strong coupling to plasmonic nanoantennas." *Science Advances* 4, no. 7 (2018)..

- [53] Balci, Sinan, Betül Kucukoz, Osman Balci, Ahmet Karatay, Coskun Kocabas, and Gul Yaglioglu. "Tunable Plexcitonic Nanoparticles: A Model System for Studying Plasmon–Exciton Interaction from the Weak to the Ultrastrong Coupling Regime." *ACS Photonics* 3, no. 11 (2016), 2010-2016.
- [54] Qing, Ye M., Yongze Ren, Dangyuan Lei, Hui F. Ma, and Tie J. Cui. "Strong coupling in two-dimensional materials-based nanostructures: a review." *Journal of Optics* 24, no. 2 (2022), 024009.
- [55] Törmä, P., and W. L. Barnes. "Strong coupling between surface plasmon polaritons and emitters: a review." *Reports on Progress in Physics* 78, no. 1 (2014), 013901.
- [56] Bekele, Dagmawi, Yi Yu, Kresten Yvind, and Jesper Mork. "Fano Resonances: In-Plane Photonic Crystal Devices using Fano Resonances (Laser Photonics Rev. 13(12)/2019)." *Laser & Photonics Reviews* 13, no. 12 (2019).
- [57] Diguna, Lina, Liliana Tjahjana, Yudi Darma, Shuwen Zeng, Hong Wang, and Muhammad Birowosuto. "Light–Matter Interaction of Single Quantum Emitters with Dielectric Nanostructures." *Photonics* 5, no. 2 (2018), 14.
- [58] Kato, Fumiya, Hiro Minamimoto, Fumika Nagasawa, Yuko S. Yamamoto, Tamitake Itoh, and Kei Murakoshi. "Active Tuning of Strong Coupling States between Dye Excitons and Localized Surface Plasmons via Electrochemical Potential Control." *ACS Photonics* 5, no. 3 (2018), 788-796.
- [59] Hobson, P.A., J.A.E. Wasey, I. Sage, and W.L. Barnes. "The role of surface plasmons in organic light-emitting diodes." *IEEE Journal of Selected Topics in Quantum Electronics* 8, no. 2 (2002), 378-386.
- [60] Fusella, Michael A., Renata Saramak, Rezlind Bushati, Vinod M. Menon, Michael S. Weaver, Nicholas J. Thompson, and Julia J. Brown. "Plasmonic enhancement of stability and brightness in organic light-emitting devices." *Nature* 585, no. 7825 (2020), 379-382.
- [61] Zhang, Yupeng, Chang-Keun Lim, Zhigao Dai, Guannan Yu, Joseph W. Haus, Han Zhang, and Paras N. Prasad. "Photonics and optoelectronics using nanostructured hybrid perovskite media and their optical cavities." *Physics Reports* 795 (2019), 1-51.
- [62] Chénais, Sébastien, and Sébastien Forget. "Recent advances in solid-state organic lasers." *Polymer International* 61, no. 3 (2011), 390-406.

- [63] Bongu, Sudhakara R., and Prem B. Bisht. "Nonlinear Optical Properties of Single Walled Carbon Nanotubes-Laser Dye System Under Picosecond Pumping." *12th International Conference on Fiber Optics and Photonics*, 2014.
- [64] Turner, Daniel B., Krystyna E. Wilk, Paul M. Curmi, and Gregory D. Scholes. "Comparison of Electronic and Vibrational Coherence Measured by Two-Dimensional Electronic Spectroscopy." *The Journal of Physical Chemistry Letters* 2, no. 15 (2011), 1904-1911.
- [65] Jansson, Tomasz P. *Tribute to Emil Wolf: Science and Engineering Legacy of Physical Optics*. Vol. 139. Bellingham, WA: SPIE Press. (2005).
- [66] J. H. Nahida, "Spectrophotometric analysis for the UV-irradiated (PMMA)," *Int. J. Basic Appl. Sci.*, vol. 12, no. 02, pp. 58–67, 2012, 58-67.
- [67] AL Hussainey, Afrah M., Ruaa K. Mahmoud, and Talib M. ALShafie. "Study the Optical and Spectral Properties of the Acridine Dye As an Effective Medium in Dye Lasers." *JOURNAL OF UNIVERSITY OF BABYLON for Pure and Applied Sciences* 26, no. 10 (2018), 167-180.
- [68] Saleh, Bahaa EA, and Malvin Carl Teich. *Fundamentals of Photonics*. Hoboken, NJ: John Wiley & Sons. (2019), 049901.
- [69] López Arbeloa, F., A. Costela, and I. López Arbeloa. "Molecular structure effects on the lasing properties of rhodamines." *Journal of Photochemistry and Photobiology A: Chemistry* 55, no. 1 (1990), 97-103.
- [70] Lazzeretti, Paolo. "Continuity equations for electron charge densities and current densities induced in molecules by electric and magnetic fields." *The Journal of Chemical Physics* 151, no. 11 (2019).
- [71] Lomon, Earle L. "Modern Applications: *Classical Electrodynamics* . John David Jackson. Wiley, New York, 1962. xvii + 641 pp. Illus. \$13." *Science* 136, no. 3521 (1962), 1046-1047.
- [72] Brown, Matthew S., and Craig B. Arnold. "Fundamentals of Laser-Material Interaction and Application to Multiscale Surface Modification." *Laser Precision Microfabrication*, 2010, 91-120.
- [73] Pálfalvi, László. A LiNbO₃ nemlineáris optikai tulajdonságainak vizsgálata Z-scan módszerrel. Ph. D. thesis, Szegedi Tudományegyetem. (2003).
- [74] Tan, Dezhi, Kaniyarakkal N. Sharafudeen, Yuanzheng Yue, and Jianrong Qiu. "Femtosecond laser induced phenomena in transparent solid materials: Fundamentals and applications." *Progress in Materials Science* 76 (2016), 154-228.

- [75] Moretti, Giacomo, Gastone P. Papini, Michele Righi, David Forehand, David Ingram, Rocco Vertechy, and Marco Fontana. "Resonant wave energy harvester based on dielectric elastomer generator." *Smart Materials and Structures* 27, no. 3 (2018), 035015.
- [76] KROLENKO, S., S. ADAMYAN, T. BELYAEVA, and T. MOZHENOK. "Acridine orange accumulation in acid organelles of normal and vacuolated frog skeletal muscle fibres." *Cell Biology International* 30, no. 11 (2006), 933-939.
- [77] Valeur, Bernard, and Mário N. Berberan-Santos. "Molecular Fluorescence." (2012).
- [78] "McWeeny, Prof. Roy, (born 19 May 1924), Professor of Theoretical Chemistry, University of Pisa, 1982–97, Professor Emeritus, since 1998." *Who's Who*, 2007.
- [79] Sahib, Nadia Hussein. "Spectroscopic Study for Some Organic Dyes." Al-Mustansiriya University, College of Sciences (2005), 173-179.
- [80] Tang, Longteng, and Chong Fang. "Photoswitchable Fluorescent Proteins: Mechanisms on Ultrafast Timescales." *International Journal of Molecular Sciences* 23, no. 12 (2022), 6459.
- [81] Lakowicz, Joseph R., ed. *Principles of Fluorescence Spectroscopy*. Springer Science & Business Media (2013).
- [82] Chantzis, Agisilaos, Javier Cerezo, Aurélie Perrier, Fabrizio Santoro, and Denis Jacquemin. "Optical Properties of Diarylethenes with TD-DFT: 0–0 Energies, Fluorescence, Stokes Shifts, and Vibronic Shapes." *Journal of Chemical Theory and Computation* 10, no. 9 (2014), 3944-3957.
- [83] Sze, Simon M., Yiming Li, and Kwok K. Ng. *Physics of Semiconductor Devices*. John Wiley & Sons (2021),
- [84] Chaiken, Joseph. "Laser Chemistry: Spectroscopy, Dynamics and Applications Edited by Helmut H. Telle (Swansea University, U.K.), Angel González Ureña (Universidad Complutense de Madrid, Spain), and Robert J. Donovan (Edinburg University, U.K.). John Wiley & Sons, Ltd.: Chichester. 2007. xiv + 502 pp. \$90.00. ISBN 978-0-471-48571-1." *Journal of the American Chemical Society* 129, no. 46 (2007), 14525-14526.
- [88] Dechun, Z. "Chemical and photophysical properties of materials for OLEDs." *Organic Light-Emitting Diodes (OLEDs)*, (2013), 114-142.
- [89] Jain, Mayank, and Lars Bötter-Jensen. "Luminescence Instrumentation." *Defect and Diffusion Forum* 357 (2014), 245-260.

- [90] Zhao, Zheng, Haoke Zhang, Jacky W. Lam, and Ben Z. Tang. "Aggregation-Induced Emission: New Vistas at the Aggregate Level." *Angewandte Chemie International Edition* 59, no. 25 (2020), 9888-9907.
- [91] Pereira, L. F. (Ed.). (2012). *Organic light emitting diodes: The use of rare earth and transition metals*. CRC Press.
- [92] Mafuné,, Fumitaka, Jun-ya Kohno, Yoshihiro Takeda, Tamotsu Kondow, and Hisahiro Sawabe. "Formation of Gold Nanoparticles by Laser Ablation in Aqueous Solution of Surfactant." *The Journal of Physical Chemistry B* 105, no. 22 (2001), 5114-5120.
- [93] Youssef, Kareem, Ying Li, Samantha O'Keeffe, Lu Li, and Qibing Pei. "Light-Emitting Conjugated Polymers: Fundamentals of Materials Selection for Light-Emitting Electrochemical Cells (Adv. Funct. Mater. 33/2020)." *Advanced Functional Materials* 30, no. 33 (2020).
- [94] Kumari, Beena. "'A REVIEW ON NANOPARTICLES: THEIR PREPARATION METHOD AND APPLICATIONS'." *Indian Research Journal of Pharmacy and Science* 5, no. 2 (2018), 1420-1426.
- [95] Khan, Waseem, Rahul Sharma, and Parveen Saini. "Carbon Nanotube-Based Polymer Composites: Synthesis, Properties and Applications." *Carbon Nanotubes - Current Progress of their Polymer Composites*, 2016.
- [96] Naz, Muhammad Y., Shazia Shukrullah, Abdul Ghaffar, Khuram Ali, and S. K. Sharma. "Synthesis and Processing of Nanomaterials." *Solar Cells*, 2020, 1-23.
- [97] Kumar, Prashant, Alan Robins, Sotiris Vardoulakis, and Rex Britter. "A review of the characteristics of nanoparticles in the urban atmosphere and the prospects for developing regulatory controls." *Atmospheric Environment* 44, no. 39 (2010), 5035-5052.
- [98] Huang, Xiaohua, Prashant K. Jain, Ivan H. El-Sayed, and Mostafa A. El-Sayed. "Gold nanoparticles: interesting optical properties and recent applications in cancer diagnostics and therapy." *Nanomedicine* 2, no. 5 (2007), 681-693.
- [99] Kalyani, N. T., Hendrik Swart, and S.J. Dhoble. "Organic Light-Emitting Diodes." *Principles and Applications of Organic Light Emitting Diodes (OLEDs)*, 2017, 141-170.
- [100] Youssef, Kareem, Ying Li, Samantha O'Keeffe, Lu Li, and Qibing Pei. "Light-Emitting Conjugated Polymers: Fundamentals of Materials Selection for Light-

- Emitting Electrochemical Cells (Adv. Funct. Mater. 33/2020)." *Advanced Functional Materials* 30, no. 33 (2020).
- [101] Sekine, Chizu, Yoshiaki Tsubata, Takeshi Yamada, Makoto Kitano, and Shuji Doi. "Recent progress of high performance polymer OLED and OPV materials for organic printed electronics." *Science and Technology of Advanced Materials* 15, no. 3 (2014), 034203.
- [102] Youssef, Kareem, Ying Li, Samantha O'Keeffe, Lu Li, and Qibing Pei. "Light-Emitting Conjugated Polymers: Fundamentals of Materials Selection for Light-Emitting Electrochemical Cells (Adv. Funct. Mater. 33/2020)." *Advanced Functional Materials* 30, no. 33 (2020).
- [103] Reineke, Sebastian, Michael Thomschke, Björn Lüssem, and Karl Leo. "White organic light-emitting diodes: Status and perspective." *Reviews of Modern Physics* 85, no. 3 (2013), 1245-1293.
- [104] Gafner, Yury, Svetlana Gafner, and Darya Bashkova. "On measuring the structure stability for small silver clusters to use them in plasmonics." *Journal of Nanoparticle Research* 21, no. 11 (2019).
- [105] Liu, Jie, Larry N. Lewis, and Anil R. Duggal. "Photoactivated and patternable charge transport materials and their use in organic light-emitting devices." *Applied Physics Letters* 90, no. 23 (2007).
- [106] Reineke, Sebastian, Michael Thomschke, Björn Lüssem, and Karl Leo. "White organic light-emitting diodes: Status and perspective." *Reviews of Modern Physics* 85, no. 3 (2013), 1245-1293.
- [107] Kalyani, N. T., Hendrik Swart, and S.J. Dhoble. "Organic Light-Emitting Diodes." *Principles and Applications of Organic Light Emitting Diodes (OLEDs)*, 2017, 141-170.
- [108] Muccini, Michele, and Stefano Toffanin. "Organic Light-Emitting Transistors." 2016.
- [109] Salem, A.M.S., S.M. El-Sheikh, Farid A. Harraz, S. Ebrahim, M. Soliman, H.S. Hafez, I.A. Ibrahim, and M.S.A. Abdel-Mottaleb. "Inverted polymer solar cell based on MEH-PPV/PC 61 BM coupled with ZnO nanoparticles as electron transport layer." *Applied Surface Science* 425 (2017), 156-163.
- [110] Groenhuis, R. A., H. A. Ferwerda, and J. J. Ten Bosch. "Scattering and absorption of turbid materials determined from reflection measurements 1: Theory." *Applied Optics* 22, no. 16 (1983), 2456.

- [111] Hamamda, Mehdi, Pierre Pillet, Hans Lignier, and Daniel Comparat. "Rotational cooling of molecules and prospects." *Journal of Physics B: Atomic, Molecular and Optical Physics* 48, no. 18 (2015), 182001.
- [112] Zare, Richard N. "My Life with LIF: A Personal Account of Developing Laser-Induced Fluorescence." *Annual Review of Analytical Chemistry* 5, no. 1 (2012), 1-14.
- [113] Winefordner, James D., Igor B. Gornushkin, Tiffany Correll, Emily Gibb, Benjamin W. Smith, and Nicol Omenetto. "Comparing several atomic spectrometric methods to the super stars: special emphasis on laser induced breakdown spectrometry, LIBS, a future super star." *Journal of Analytical Atomic Spectrometry* 19, no. 9 (2004), 1061.
- [114] Saleh, Bahaa EA, and Malvin Carl Teich. *Fundamentals of Photonics*. John Wiley & Sons (2019).
- [115] Neusser, H. J. "S. A. Losev: Gasdynamic Laser, Vol. 12 aus der Reihe: Springer Series in Chemical Physics, Springer-Verlag, Berlin, Heidelberg, New York 1981. 310 Seiten, Preis: \$ 53,40." *Berichte der Bunsengesellschaft für physikalische Chemie* 85, no. 12 (1981), 1165-1165.
- [116] D. M. Hercules, "Fluorescence & Phosphorescence Analysis", Inter Science Publisher a division of John Wiley & Sons. New York. London. Sydney. (1960). 639-640.
- [117] Fukuda, Makoto, and Keiichi Mito. "Solid-State Dye Laser with Photo-Induced Distributed Feedback." *Japanese Journal of Applied Physics* 39, no. 10R (2000), 5859.
- [118] Nickel, Bernhard. "Luminescence Spectroscopy. Herausgegeben von M. D. Lumb. Academic Press, New York 1978. IX, 375 S., geb. \$ 49.75." *Angewandte Chemie* 91, no. 12 (1979), 1032-1032.
- [119] Al-Thib, Anwar T., Nisreen K. Al-Alwi, and Ali. S. Eliwe. "Spectroscopic and Thermodynamic Studies of Charge- Transfer Complexes Formation Between Cytosine, Uracil and Thymine With Electronic Acceptors." *Journal of Al-Nahrain University Science* 16, no. 2 (2013), 37-45.
- [120] Halip, Hafizah, Yuto Yoshimura, Wataru Inami, and Yoshimasa Kawata. "Ultrashort laser based two-photon phase-resolved fluorescence lifetime measurement method." *Methods and Applications in Fluorescence* 8, no. 2 (2020), 025003.

- [121] Naheda Hamood Abd Garaah , " Study Absorption Spectra and Fluorescence Of Some Organic Dyes In Dye Laser " , A Thesis , University of Babylon , College of Science , (2011). 164-175.
- [122] Jabbar, Abber A., Sabah L. Alwan, and Zaidan K. Imran. "Survey Of Fusarium Verticillioides Associated With Maize (Zea Mays L.) In Iraq." *International Journal Of Medical Science And Clinical Invention*, 2015.
- [123] Nad, Sanjukta, and Haridas Pal. "Photophysical Properties of Coumarin-500 (C500): Unusual Behavior in Nonpolar Solvents." *The Journal of Physical Chemistry A* 107, no. 4 (2003), 501-507.
- [124] Kadhim S AL-Dhahiry, Jawad, Tarik Khalid AL Niamey, Ameer Kadhum Daher, Ramzi Kadhum AL, and A. Biati. "PENDRED'S SYNDROME; A CASE REPORT AND REVIEW OF LITERATURES." *The Medical Journal of Basrah University* 29, no. 1 (2011), 39-42.
- [125] Ahamed Kadem Kodeary," Study Fluorescence Of Some Dyes rhodamine 6G and rhodamine B", A Thesis, University of Babylon , College of Science , (2015),373-379.
- [126] Sara Jawad Shoja," Study of Spectroscopic and optical Properties for phenolphthalein dye as a laser active medium", University of Babylon, College of Science for Women, (2016),11-18.
- [127] Baranowski, Thomas, Thomas Dreier, Christof Schulz, and Torsten Endres. "Excitation wavelength dependence of the fluorescence lifetime of anisole." *Physical Chemistry Chemical Physics* 21, no. 27 (2019), 14562-14570.
- [128] Kim, Heedae, Jong S. Kim, and Inhong Kim. "Radiative decay time as a function of temperature in double GaAs quantum rings." *Applied Surface Science* 478 (2019), 487-491.
- [129] H.S., Geethanjali, R.M. Melavanki, Nagaraja D., Bhavya P., and R.A. Kusanur. "Binding of boronic acids with sugars in aqueous solution at physiological pH - Estimation of association and dissociation constants using spectroscopic method." *Journal of Molecular Liquids* 227 (2017), 37-43.
- [130] Li, Yungui, Bas Van der Zee, Gert-Jan A. Wetzelaer, and Paul W. Blom. "Optical Outcoupling Efficiency in Polymer Light-Emitting Diodes." *Advanced Electronic Materials* 7, no. 6 (2021).
- [131] Yasir, Mohammad, Tianqi Sai, Alba Sicher, Frank Scheffold, Ullrich Steiner, Bodo D. Wilts, and Eric R. Dufresne. "Enhancing the Refractive Index of Polymers with a Plant-Based Pigment." *Small* 17, no. 44 (2021).

- [132] Hu, Jun, Yinuo Wang, Qiang Li, Shiyang Shao, Lixiang Wang, Xiabin Jing, and Fosong Wang. "Hyperfluorescent polymers enabled by through-space charge transfer polystyrene sensitizers for high-efficiency and full-color electroluminescence." *Chemical Science* 12, no. 39 (2021), 13083-13091.
- [133] Zhang, Zekun, Rui Tian, Daolei Lin, Dezhen Wu, Chao Lu, and Xue Duan. "Three-Dimensional Fluorescent Imaging to Identify Multi-Paths in Polymer Aging." *Analytical Chemistry* 93, no. 29 (2021), 10301-10309.
- [134] Li, Zhenye, Wenkai Zhong, Lei Ying, Feng Liu, Ning Li, Fei Huang, and Yong Cao. "Morphology optimization via molecular weight tuning of donor polymer enables all-polymer solar cells with simultaneously improved performance and stability." *Nano Energy* 64 (2019), 103931.
- [135] Winterton, Neil. "The green solvent: a critical perspective." *Clean Technologies and Environmental Policy* 23, no. 9 (2021), 2499-2522.
- [136] Mahata, T., A. Mandal, and V.R. Dantham. "Role of composition and size-dependent damping due to electron-surface scattering on plasmonic properties of gold-silver alloy nanoparticles: A theoretical study." *Journal of Quantitative Spectroscopy and Radiative Transfer* 276 (2021), 107940.
- [137] Ou, Xiaowen, Yuqi Liu, Mingxing Zhang, Li Hua, and Shenshan Zhan. "Plasmonic gold nanostructures for biosensing and bioimaging." *Microchimica Acta* 188, no. 9 (2021).
- [138] Ramalingam, Vaikundamoorthy, and Rajendran Rajaram. "A paradoxical role of reactive oxygen species in cancer signaling pathway: Physiology and pathology." *Process Biochemistry* 100 (2021), 69-81.
- [139] Morozova, Olga V. "Silver Nanostructures: Limited Sensitivity of Detection, Toxicity and Anti-Inflammation Effects." *International Journal of Molecular Sciences* 22, no. 18 (2021), 9928.
- [140] Yonesato, Kentaro, Seiji Yamazoe, Daisuke Yokogawa, Kazuya Yamaguchi, and Kosuke Suzuki. "A Molecular Hybrid of an Atomically Precise Silver Nanocluster and Polyoxometalates for H₂ Cleavage into Protons and Electrons." *Angewandte Chemie International Edition* 60, no. 31 (2021), 16994-16998.
- [141] Brett, Calvin J., Wiebke Ohm, Björn Fricke, Alexandros E. Alexakis, Tim Laarmann, Volker Körstgens, Peter Müller-Buschbaum, L. D. Söderberg, and Stephan V. Roth. "Nanocellulose-Assisted Thermally Induced Growth of Silver Nanoparticles for Optical Applications." *ACS Applied Materials & Interfaces* 13, no. 23 (2021), 27696-27704.

- [142] Al-Bati, Sameer, Mohammad H. Hj. Jumali, Bandar A. Al-Asbahi, Khatatbeh Ibtehaj, Chi C. Yap, Saif M. Qaid, Hamid M. Ghaithan, and W. A. Farooq. "Improving Photophysical Properties of White Emitting Ternary Conjugated Polymer Blend Thin Film via Additions of TiO₂ Nanoparticles." *Polymers* 12, no. 9 (2020), 2154.
- [143] Boriskina, Svetlana V., Hadi Ghasemi, and Gang Chen. "Plasmonic materials for energy: From physics to applications." *Materials Today* 16, no. 10 (2013), 375-386.
- [144] Guo, Jhao-Yu, Jou-An Chen, Song-Yu Chen, Meng-Lun Lee, Wei-Ren Liu, and Yu-Lin Kuo. "Reactive plasma oxygen-modified and nitrogen-doped soft carbon as a potential anode material for lithium-ion batteries using a tornado-type atmospheric pressure plasma jet." *Electrochimica Acta* 427 (2022), 140897.
- [145] Martin, S. J., D. D. Bradley, P. A. Lane, H. Mellor, and P. L. Burn. "Linear and nonlinear optical properties of the conjugated polymers PPV and MEH-PPV." *Physical Review B* 59, no. 23 (1999), 15133-15142.
- [146] Qin, Ting, and Alessandro Troisi. "Relation between Structure and Electronic Properties of Amorphous MEH-PPV Polymers." *Journal of the American Chemical Society* 135, no. 30 (2013), 11247-11256.
- [147] Kim, Jong G., Ji H. Kim, Byung-Jin Song, Chul W. Lee, and Ji S. Im. "Synthesis and its characterization of pitch from pyrolyzed fuel oil (PFO)." *Journal of Industrial and Engineering Chemistry* 36 (2016), 293-297.
- [148] Ariu, M., D.G Lidzey, and D.D.C Bradley. "Influence of film morphology on the vibrational spectra of dioctyl substituted polyfluorene (PFO)." *Synthetic Metals* 111-112 (2000), 607-610.
- [149] Ye, Zhiping, Jean-Marc Giraudon, Nathalie De Geyter, Rino Morent, and Jean-François Lamonier. "The Design of MnO_x Based Catalyst in Post-Plasma Catalysis Configuration for Toluene Abatement." *Catalysts* 8, no. 2 (2018), 91.
- [150] Li, Yuyang, Jianghuai Cai, Lidong Zhang, Tao Yuan, Kuiwen Zhang, and Fei Qi. "Investigation on chemical structures of premixed toluene flames at low pressure." *Proceedings of the Combustion Institute* 33, no. 1 (2011), 593-600.
- [151] Abdulhalim, Ibrahim. "Coupling configurations between extended surface electromagnetic waves and localized surface plasmons for ultrahigh field enhancement." *Nanophotonics* 7, no. 12 (2018), 1891-1916.

- [152] Weston, R. E., and G. W. Flynn. "Relaxation of Molecules with Chemically Significant Amounts of Vibrational Energy: The Dawn of the Quantum State Resolved Era." *Annual Review of Physical Chemistry* 43, no. 1 (1992), 559-589.

الخلاصة

البوليمرات الباعثة للضوء (LEPs) هي مواد تمتص الضوء عند طول موجي معين وتصدره عند طول موجي آخر، وهي ضرورية لتطبيقات مثل مصابيح LED وشاشات العرض. يؤدي خلط LEPs مع الجسيمات النانوية المعدنية البلازمونية إلى تعزيز خصائصها البصرية من خلال اقتران البلازمون والإكسيتون. تعمل هذه الظاهرة على تعزيز كفاءة انبعاث الضوء، وتسمح بالتحكم الدقيق في الضوء المنبعث، وتحسن الأداء العام للجهاز الإلكتروني البصري.

ركزت الدراسة التجريبية الحالية على تحسين الخواص البصرية البوليمرات الباعثة للضوء عن طريق مزجها بالجسيمات النانوية المعدنية البلازمونية. لتحقيق هذا الغرض، يتم استخدام نوعين من البوليمرات الباعثة للضوء (MEH-PPV و PFO) والتي يتم حلها مع مذيب عضوي يدعى (التولوين) بتركيزات مختلفة. بالإضافة إلى ذلك، تم تصنيع جسيمات الذهب النانوية و جسيمات الفضة النانوية بطريقة القشط بالليزر النبضي في السوائل مع نبضات ليزر النانو ثانية عند 1064 نانومتر. متوسط حجم الجسيمات النانوية والتي تم انتاجها تجريبياً من 18 إلى 35 نانومتر.

للحصول على خصائص بصرية محسنة، يتم خلط بوليمر MEH-PPV مع جسيمات الذهب النانوية بتركيزات مختلفة، بينما يتم خلط بوليمر PFO مع جسيمات الفضة النانوية بتركيزات مختلفة. تم قياس الامتصاص البصري باستخدام مقياس الطيف الضوئي (UV-Vis) وكذلك مقياس الطيف الفلور، وتقنية الفلور المستحثة بالليزر (LIF) لجميع العينات. كشفت النتائج عن خصائص بصرية قابلة للضبط والتعديل لكلا النوعين المستخدم من البوليمرات الباعثة للضوء من خلال التحكم في تركيز الجسيمات النانوية التي تضاف لها.

وبناء على ذلك، أظهرت النتائج إمكانية البوليمرات الباعثة للضوء الممزوجة بالجسيمات النانوية البلازمونية في العديد من التطبيقات، وخاصة في تطوير الأجهزة البصرية والكاشفات.

وقد لوحظ الانبعاث الأمثل عند تركيز الجسيمات النانوية بمقدار 500 ميكرومتر. تكشف دراستنا عن تغييرات كبيرة في خصائص انبعاث الضوء لبوليمر MEH-PPV عند إدخال جسيمات الذهب النانوية، خاصة في أطراف LIF عند طول موجة إثارة يبلغ 532 نانومتر. وهذا يؤكد التفاعل المعقد بين جسيمات الذهب النانوية ومصفوفة البوليمر، مما يعزز فهمنا لتأثيرات اقتران الإكسيتون والبلازمون في هذا النظام المركب النانوي.



جمهورية العراق
وزارة التعليم العالي والبحث العلمي
جامعة بابل
كلية علوم النبات
قسم فيزياء الليزر

دراسة تأثير البلازمون السطحي على الخواص البصرية للبوليمرات الباعثة للضوء

رسالة

مقدمة الى قسم فيزياء الليزر وتطبيقاته في كلية العلوم للنبات / جامعة بابل وهي جزء من متطلبات نيل
درجة الماجستير في علوم فيزياء الليزر

من قبل

زينب عدنان عبد المهدي

بكالوريوس علوم فيزياء الليزر 2019

بإشراف

أ.م.د. أحمد كاظم خضير

أ.م.د. نزار سالم شنان